Non-cyanobacterial diazotrophs from the Rhizobiales order support marine microalgae in nitrogen-depleted environments

Udita Chandola[1], Marinna Gaudin[2,3], Camille Trottier[1], Louis Josselin Lavier Aydat[1], Eric Manirakiza[1], Samuel Menicot[1], Erik Jörg Fischer[4], Isabelle Louvet[5], Thomas Lacour[6], Timothée Chaumier[1], Atsuko Tanaka[7], Georg Pohnert[4], Samuel Chaffron[2,3] and Leïla Tirichine[1,8*]

[1] Nantes Université, CNRS, US2B, UMR 6286, F-44000 Nantes, France.

[2] Nantes Université, École Centrale Nantes, CNRS, LS2N, UMR 6004, Nantes, France.

[3] Research Federation for the Study of Global Ocean Systems Ecology and Evolution, FR2022/Tara Oceans GOSEE, F-75016 Paris, France.

[4] Friedrich-Schiller-Universitet Jena, Institute for Inorganic and Analytical Chemistry, Lessingstrasse 8, 7743, Jena, Germany

[5] Nantes Université, CNRS, CEISAM, UMR 6230, F-44000 Nantes, France.

[6] Ifremer, PHYTOX, PHYSALG, Rue de l'Ile d'Yeu, BP21105, Nantes Cedex 03, 44311, France

[7] Department of Chemistry, Biology and Marine Science, Faculty of Science, University of the Ryukyus, Okinawa 903-0213, Japan

[8] Institute for Marine and Antarctic Studies (IMAS), Ecology and Biodiversity Centre, University of Tasmania, Hobart, TAS, 7004, Australia

[*]Correspondence: tirichine-l@univ-nantes.fr; Tel.: +33-276645058

Abstract

Background

Non-cyanobacteria diazotrophs (NCDs) were shown to dominate in surface waters shifting the long-held paradigm of cyanobacteria dominance and raising fundamental questions on how these putative heterotrophic bacteria thrive in sunlit oceans. The absence of laboratory cultures of these bacteria significantly limits our ability to understand their behavior in natural environments and, consequently, their contribution to the marine nitrogen cycle.

Results

Here, we used a multidisciplinary approach and report an unprecedented finding in the diatom *Phaeodactylum tricornutum* (*Pt*) of NCDs in the phycosphere or the pelagic community sustaining its survival in the absence of bioavailable nitrogen. We sequenced the bacterial metacommunity associated with Pt and assembled several bacterial genomes, identifying multiple NCDs from the Rhizobiales order, including *Bradyrhizobium*, *Mesorhizobium*, *Georhizobium* and *Methylobacterium*. We demonstrated the nitrogen-fixing ability of PtNCDs through in silico identification of nitrogen fixation genes, or by using PCR, acetylene reduction, or 15N incorporation. We showed the wide occurrence of this type of interactions with the isolation of NCDs from other microalgae, their identification in the environment, and their predicted associations with photosynthetic microalgae.

Conclusions

Our study underscores the importance of microalgae interactions with NCDs to permit and support nitrogen fixation. This work provides a unique model Pt-NCDs to study the ecology of this interaction advancing our understanding of the key drivers of global marine nitrogen fixation.

Keywords: Biological nitrogen fixation, non-cyanobacterial diazotrophs, Rhizobiales, *Phaeodactylum tricornutum*, microalgae, eukaryote-prokaryote interactions

Background

Nearly 80% of Earth's atmosphere is in the form of molecular nitrogen (N_2). Similarly, the main form of nitrogen in the oceans which cover 71% of Earth surface is dissolved dinitrogen. The rest is reactive nitrogen in the form of nitrate, ammonia and dissolved organic compounds, which are very scarce, rendering nitrogen one of the main limiting factors of productivity in most areas of the oceans [1]. Despite its dominance, ironically, N_2 is unavailable for use by most organisms. Biological nitrogen fixation which is an energy intensive process is specific to only some prokaryotes and archaea termed diazotrophs. It is catalyzed by the nitrogenase enzyme complex including the nitrogenase reductase encoded by the *nifH* gene and the nitrogenase composed of two pairs of different subunits, α and β, respectively encoded by the *nifD* and *nifK* genes [2]. Therefore, eukaryotes are only able to obtain fixed nitrogen through their interactions with diazotrophs [3], although recent evidence has revealed the evolutionary conversion of a cyanobacterium into a nitrogen-fixing organelle within its host, representing the first documented case of nitrogen fixation in a eukaryote [4].

In aquatic habitats, associations between diazotrophic cyanobacteria such as Richelia/Calothrix and various eukaryotes, including several diatom genera such as *Chaetoceros, Rhizosolenia* and *Hemiaulus* known as diatom-diazotroph associations are common and important in oligotrophic habitats of the ocean [5]. Because the nitrogenase complex is sensitive to oxygen, diazotrophs evolved protective nitrogen fixation alternatives that involve conditionally, temporally, or spatially separating oxidative phosphorylation or photosynthesis from nitrogen fixation [6-11]. Cyanobacteria were considered for a very long time as the main diazotrophs in the ocean. However, recent molecular analyses indicated that non-cyanobacterial diazotrophs (NCDs) are also present and active, exhibiting an important presence of diverse *nifH* genes related to non-cyanobacteria, especially to Proteobacteria and Planctomycetes [12-16].

The overwhelming dominance of NCDs raises important questions on how these presumably heterotrophs proteobacteria thrive in the photic zones of the oceans. One emerging hypothesis is that their association with aggregates and larger cellular fractions including phytoplankton, may provide the optimal conditions for nitrogen fixation [16-19]. In our work, we provide evidence for the occurrence of associations between free-living NCDs and several microalgae. More importantly, we identified this interaction in an attractive biological model, the diatom *Phaeodactylum tricornutum (Pt),* opening important and unique opportunities to investigate the molecular mechanisms of diazotrophy in symbiotic interactions in microalgae.

We sequenced the bacterial meta-community associated with *Pt* and identified previously unknown diverse marine diazotrophs of mainly Alphaproteobacteria type, supporting the survival of host cells in the absence of any form of usable nitrogen. Further, we isolated, cultured, sequenced and fully assembled some of the Pt-associated NCDs. Their assembled genomes clustered phylogenetically to NCDs found in the environment and showed environmental co-occurrence patterns with microalgae including diatoms, green algae and haptophytes. Interestingly, most of PtNCDs belong to the Rhizobiales, order known to nodulate legumes. These NCDs include *Bradyrhizobium*, *Rhizobium*, *Mesorhizobium*, *Methylobacterium*, *Phylobacterium* and *Georhizobium* raising important questions into the evolution of symbiotic nitrogen fixation and its terrestrial or marine origins. Our findings differ from a recent study that identified an NCD residing within a diatom as an obligate symbiont with a reduced genome compared to free living NCDs [20]. Our work brings evidence for an apparently prevalent interaction between microalgae and NCDs, that might explain how both partners cope with periods of nitrogen scarcity, and how these NCDs compromise for nitrogen fixation with its high energy cost in fully oxygenated areas of the water column. These new findings will have to be considered in future nitrogen and carbon biogeochemical cycling studies.

Results

Identification of non-cyanobacterial diazotrophs interaction with diatoms

In a screening of 10 xenic environmental samples of Pt grown in nitrogen-depleted medium, one accession *P. tricornutum 15* (hereafter *Pt15*), sampled from East China sea, was found to survive in contrast to the axenic control (**Fig. 1A**). This suggests that diatom growth may have been supported by bacterial nitrogen fixation providing a usable source of nitrogen to diatom cells. After 3 months of nitrogen starvation, xenic *Pt15* showed similar growth to non-starved cells upon transfer to nitrate replete medium. This indicated that *Pt15* starved cells remained viable and capable of growth under favorable conditions as evidenced by the presence of brown-pigmented cells (**Fig. 1B**). To demonstrate nitrogen fixation, we used the widely applied Acetylene Reduction Assay (ARA) [21] which detected ethylene production in nitrogen-starved xenic *Pt15* cultures. Although the ethylene levels were low, they were notably higher than those in the *E. coli* negative control, where no ethylene production was detected. Xenic *Pt15* cultures under nitrogen-replete conditions (+N) did not show any ethylene production. No ethylene was detected in axenic *Pt15* confirming that the measured ethylene

was not endogenous to the diatom cells but originated from bacterial nitrogen fixation **(Table S1**).

Fig. 1. Macro/microscopic phenotype of *P. tricornutum* cells under nitrate starvation

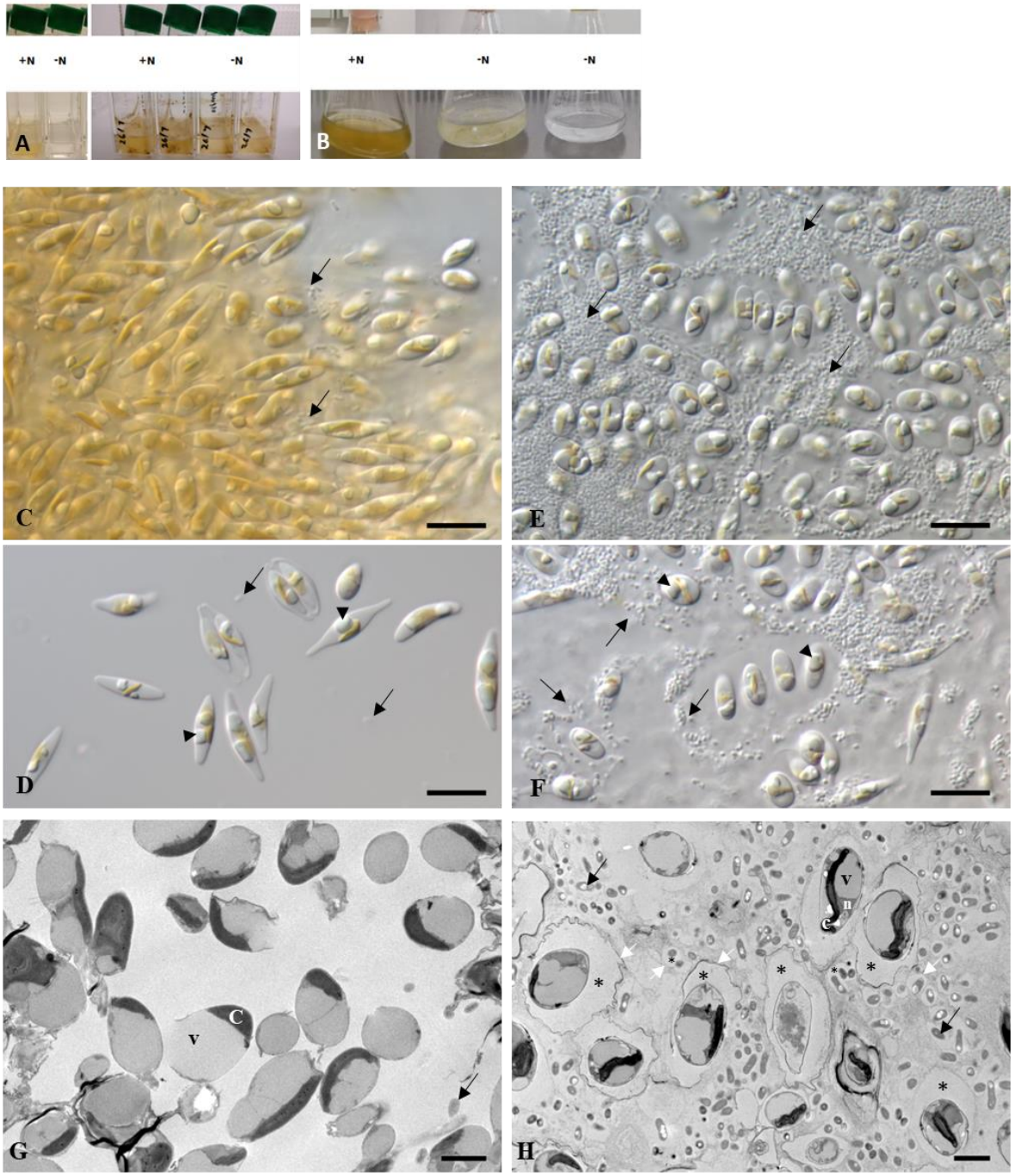

A. An illustration comparing the screening results of two *P. tricornutum* accessions: xenic *Pt4* (left), which thrives in +N but does not survive in -N, and the candidate accession, xenic *Pt15* (right), shown in duplicates. B, from right to left: axenic *Pt15* not surviving in -N (negative control), xenic *Pt15* in -N condition and xenic *Pt15* transferred to +N medium after 3 months in -N. C-H, micrographs of *P. tricornutum* xenic cultures on plates. Cells were grown in -N (E, F, H) or +N culture plates (C, D, G). Living cells were observed by DIC (C-F), and fixed cells by transmission electron microscopy (G, H). D, Diatom cells grown in +N possessed yellow-brown color of photosynthetic pigments. Mainly in aggregated cells of fusiform and oval shapes, some bacteria were observed

(arrows). D, Single or multiple whitish droplets, oil bodies, were developed next to chloroplasts (arrowheads). E, F, Diatom cells formed aggregates with a significant number of surrounding bacteria (arrows) in the -N culture, compared to the +N condition. F, Diatom cells grown without nitrate also developed oil bodies in the oval cells. G, H, Electron micrographs indicate cross-sectioned cells with or without nitrate. Organelles with high electron density are chloroplast, and major spaces were occupied by oil bodies or vacuoles, which showed low electron densities. Number of bacteria cells (arrows) were obviously larger in -N (H) compared to +N culture (G). H, Interestingly, both *Pt* cells and some bacteria are encased in sacs surrounded with a likely EPS made membrane (white arrows) which showed darker electron density around diatom cells compared to bacteria. Cells in 1G and 1H were stained with TI blue stain, which binds to negatively charged components such as anionic polysaccharides increasing electron density. A low electron density space (stars) separates *Pt* cells and bacteria from the membrane. c, chloroplast, v, vacuole, n, nucleus. Scale bars, 10 μm (C-F) and 2 μm (G, H).

To further investigate nitrogen fixation in minus N condition (-N), we measured Particulate Organic Nitrogen quota (PON) in diatom cells and showed a stable level of PON even after 80 days of growth, supporting the maintenance of diatom cells with the amounts of usable nitrogen likely provided by *Pt15* associated bacteria (**Figure S1A, Table S1**). Simultaneously, measured biomass of *Pt15*, indicated a stable cell population suggesting a ground state photosynthetic activity that might support the energy demand of nitrogen fixation (**Figure S1B**). We measured a diatom cell density of 4.3 million cells/ml in the +N condition, whereas in the -N condition, *Pt15* cell density did not exceed 360,000 cells/ml.

It is important to highlight that the growth conditions are extreme, with no nitrate supplied to diatom cells, likely leading to a slowdown in their metabolism to endure the severe conditions. Fixed nitrogen is the sole nitrogen source available to both the diatom and the entire bacterial community, likely resulting in competition for fixed nitrogen. Taken together, our results suggest bacterial nitrogen fixation activity that maintain diatom population cells stable and alive. Light microscopy showed a significant accumulation of bacteria in -N compared to +N condition. This accumulation is not an artifact but is likely a response to nitrate starvation, driven by the formation of biofilm-like clusters of NCDs. These clusters may promote the development of low-oxygen microenvironments favorable for nitrogen fixation (**Fig. 1A, D, E and F**). Bacteria were found surrounding diatom cells in the phycosphere, and not residing inside the cells. Transmission electron microscopy confirmed these observations and revealed a peculiar structure with a higher electron density around diatom cells looking like a pellicle of exopolysaccharides exclusively present in starved cells (**Fig. 1G and H**). Similar structures, although less prominent occurred around some of bacterial cells, either as a single bacterium or a group of several bacteria. The probability that these structures are composed of

polysaccharides is supported by the TI blue stain, a well-known dye that has an affinity for staining polysaccharides [22].

To identify species composition of *Pt15* bacterial community in -N and +N conditions, bacterial DNA was extracted and shotgun sequenced revealing a total of 153,4 million reads. Using the GTDB reference database, we identified a total of 2 classes, 12 families, 8 orders and 90 genera. Upon comparison of the two conditions, our analysis identified 90 distinct genera and 3,224 bacterial species in the -N condition, whereas only 18 genera and 1,540 species were detected in the +N condition. At class level, Alphaproteobacteria represented 98% ± 0,8 SD in +N and 99% ± 0,5 SD in -N, based on relative abundance estimations, while *Gammaproteobacteria* were detected with a relative abundance below 1% (**Fig. 2A**). At family level, *Sphingomonadaceae* and *Rhizobiaceae*, both known to contain diazotrophic species, dominated (**Fig. 2C**). Attached bacteria may be underrepresented due to the filtration process used to separate diatom cells from bacteria prior to DNA extraction. However, to maximize the recovery of both attached and free-living bacteria, diatom cells were vigorously vortexed multiple times before filtration.

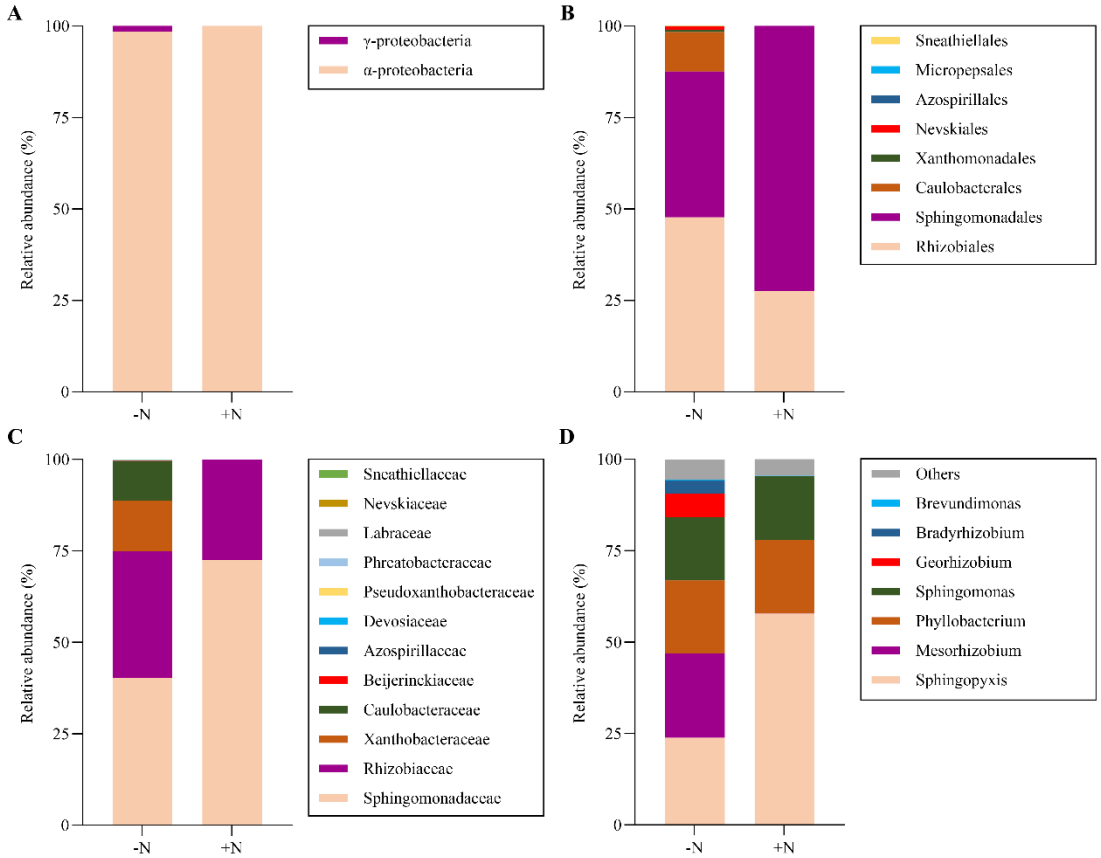

Fig. 2. Comparative relative abundance estimation of *Pt15* associated bacteria

Relative abundance of bacterial community is shown as A, class, B, order, C; family and D, genus (7 most abundant) levels between -N and +N conditions. Taxonomic assignation of metagenomic community associated to *P. tricornutum* in nitrate-deplete and nitrate-replete conditions was done using Anvio version 7.2 standard recommended pipeline using GTDB (The Genome Taxonomy Database) for assigning taxa with the in-built HMM of 22 single copy core genes [23].

At genus level, among the 90 distinct taxa identified, 73 genera were only detected in -N with no reads in +N (**Table S2**). At the genus level, the microbiome composition of the community showed a dominance of *Sphyngopixys* in +N, while -N showed a significant enrichment in *Mesorhizobium sp.*, *Bradyrhizobium sp.*, *Georhizobium sp.*, and *Brevundimonas sp*. These genera are recognized as nitrogen-fixing taxa in terrestrial environments, either existing as free-living organisms and/or forming symbiotic relationships with legumes (**Fig. 2D**). Compared to +N, *Sphyngopixys* abundance decreased in -N although its dominance over the other taxa persisted under this condition. A total of 5 *nifH* genes were detected and assigned to 4 different MAGs (MAG21-Bradyrhizobium: 2 *nifH*, MAG8-Bradyrhizobium: 1 *nifH*, MAG4-Georhizobium: 1 *nifH*, and MAG5-Sphingopyxis: 1 *nifH*) from the -N bacterial

community. No *nifH* genes were detected in the +N condition. Interestingly, several presumably non-nitrogen fixing species (67 out of 73) were significantly enriched in -N (**Table S2**), suggesting a role of these species in direct or indirect interactions within the bacterial community and/or with the host. These associated non-diazotrophic bacteria, which are enriched in the absence of bioavailable nitrogen, may contribute to the interaction through various mechanisms. We hypothesize that they could modulate competition among diazotrophs interacting with the host, produce compounds that promote microalgae growth, and inhibit antagonistic organisms, thereby facilitating the interaction with the host. However, these proposed mechanisms have yet to be demonstrated.

Isolation/identification of *P. tricornutum* associated non-cyanobacterial diazotrophs

Given the unique nature of the identified interaction involving a model diatom species and NCDs, it was important to isolate the diazotrophic bacteria identified *in silico* from metagenomics (MetaG) data in order to further explore this interaction. We used selective media and took advantage of the species assignation provided by MetaG to target the isolation of the desired bacteria according to literature reports [24-27]. Therefore, different growth conditions (media, temperature) were tested (**Additional File 1**) leading to the isolation of 9 axenic bacterial species (**Table 1**).

Table 1. List of isolated bacteria from xenic *Pt15* in -N condition.

Genus	MAG No.	Size (Mbp)	No. of contigs	*nifH* PCR identification	*nifH in silico* identification	Growth on NFM	Predicted plasmids
Mesorhizobium	**MAG3**	6.85	75	No	Yes	Yes	Yes
Bradyrhizobium sp1*.	**MAG21**	8.42	5	Yes	Yes	Yes	No
Sphingopyxis sp2	MAG7	5.00	23	ND	No	ND	Yes
Rhizobium sp.	NA	ND	ND	ND	ND	Yes	ND
Paracoccus sp.,	NA	ND	ND	ND	ND	Yes	ND
Methylobacterium*	NA	ND	ND	Yes	Yes	Yes	ND
Arthrobacter	MAG14	3.46	12	No	No	ND	ND
Pseudoarthrobacter	NA	ND	ND	No	ND	No	ND
Micrococcacea	NA	ND	ND	No	ND	No	ND

NCDs are indicated in bold. NA, not assembled, ND, not determined. * 15N incorporation was used for nitrogen fixation detection

Bacterial colonies were identified using either full length 16S rRNA gene or two hypervariable regions of the 16S (V1V2, V3V4). The presence of *nifH* was assayed using degenerate primers (**Figure S2, A and B**). Six bacteria were identified as nitrogen fixers based on a combination of *nifH* PCR amplification and/or *nifH in silico* detection along with observation of growth on nitrogen free medium for those that were isolated (**Table 1 and Table S3**). The whole set of *nif* genes including the *nifHDK* operon were identified in *Bradyrhizobium* MAG21, the only bacterium that was sequenced as a single species, while the other MAGs were assembled from

MetaG data. Among the nine isolated bacteria, some species were not detected in metagenomics sequences likely due to its low abundance, emphasizing the importance of combining sequencing and isolation/culturing approaches (**Table 1**). Due to the use of selective culturing media for bacterial species isolation, we identified species that were not necessarily present in the in-silico analysis of the metacommunity, which was grown under a single condition.

To provide stronger support for nitrogen fixation, we monitored $^{15}N_2$ gas-incorporation using mass spectrometry. This allowed a direct measure of nitrogen fixation in the two first isolated bacteria, *Bradyrhizobium* MAG21 and *Methylobacterium*. The labeling of various amino acids indicated substantial $^{15}N_2$ gas assimilation in both bacteria as well as the positive controls *Pseudomonas stutzeri* and *Azotobacter vinalendii*, while the negative controls, (the axenic *Pt15* and *Escherichia coli*) did not show any nitrogen fixation (**Table S1**). Our high-resolution LC-MS approach precisely detects the label at the molecular level through isotope-resolved ions, enabling structure-resolved detection of labeled compounds. This allows for more accurate identification of 15N2 incorporation patterns, which would be harder to resolve with bulk detection methods. This detection unequivocally establishes the nitrogen-fixing capability of the *Pt15*-associated bacteria, namely *Bradyrhizobium* and *Methylobacterium*. We could not observe $^{15}N_2$ incorporation in xenic *Pt15* cells, which can be attributed to their lower bacterial population density when compared to the lab cultured high biomass of *Bradyrhizobium* and *Methylobacterium*, as well as the competition with other numerous bacteria (~ 100 species) for fixed nitrogen. To verify that the ability of *Pt15* cells to uptake bioavailable nitrogen was not altered, we cultured xenic *Pt15* in artificial seawater containing L-valine labeled with ^{15}N, both in the presence and absence of nitrate. The analysis of endometabolomes using LC-MS distinctly revealed the incorporation of labeled valine in xenic *Pt15* when nitrate levels were at 0 µM (**Table S1**). However, no such incorporation was observed in diatom cells when nitrate was present in the medium (545 µM). This suggests that *Pt15* is able to take up nitrogen in form of amino acids from the associated NCDs, if available nitrogen is otherwise limited.

Diazotrophic MAGs are diverse and affiliated to environmentally sampled diazotrophs of Alphaproteobacteria type

To gain insights into *Pt15* associated diazotrophs and their phylogenetic relationship with known taxa, we assembled their genomes and recovered several MAGs with completeness exceeding 97% (**Table S3**). To achieve a better identification of the bacterial genetic material, we sought to recover plasmids from non-assembled reads, which are important elements for bacteria survival susceptible to contain nitrogen fixation genes. We used three different plasmid

prediction tools and recovered 42 plasmids assigned to different bacterial species with an average length of 97013 bp (**Table S3).** Besides *nifH*, several additional *nif* genes were detected in most of the MAGs, among which two were found in plasmids, *nifU* and *nifS*.

Fig. 3. Phylogenetic tree of *Pt15* assembled bacterial genomes amongst 1888 TARA bacterial MAGs and MAGs from MicroScope.

The phylogeny of 71 single copy core genes was built using Anvio platform. The upper circle represents a global view of the phylogeny built using a total of 1927 MAGs and genomes (1888 TARA MAGs, 30 terrestrial MAGs and 9 Pt15 MAGs). The bootstrap values represented from 0 – 1 with replicates of 100 and complete phylogeny can be accessed as an interactive at: https://ncdstree.univ-nantes.fr. The lower part of the figure represents a partial zoom-in on the two clusters where the Pt15 MAGs form groups in the tree with respect to other MAGs and genomes. Cluster A, left (blue highlighted text on the tree) consists of *Pt15* associated MAGs: MAG9, MAG4, MAG3, MAG2, MAG8 and MAG21. Cluster B, right (red highlighted text on the tree) consists of *Pt15* associated MAGs: MAG7, MAG5 and MAG6. Green highlighted text represents terrestrial bacteria, purple highlighted text represents diazotroph TARA MAGs (reported *nifH* gene in silico) and non-highlighted text/white background represents non-diazotroph TARA MAGs. Symbol legends, right lower-end denote information with bacterial genomes/MAGs on the tree. (Orange, oval): *Pt15* MAGs, (purple, oval): TARA diazotrophic genomes (green oval): MicroScope genomes, (brown, circle): terrestrial bacteria, (blue, circle): marine bacteria, (triangle): symbiotic, (box): free-living, (star): symbiotic and free-living, (inverted triangle): symbiotic and poor- or non-fixer and (circle): no diazotrophic information available. The numbers indicated on the oval symbols correspond to genome information in Table S6.

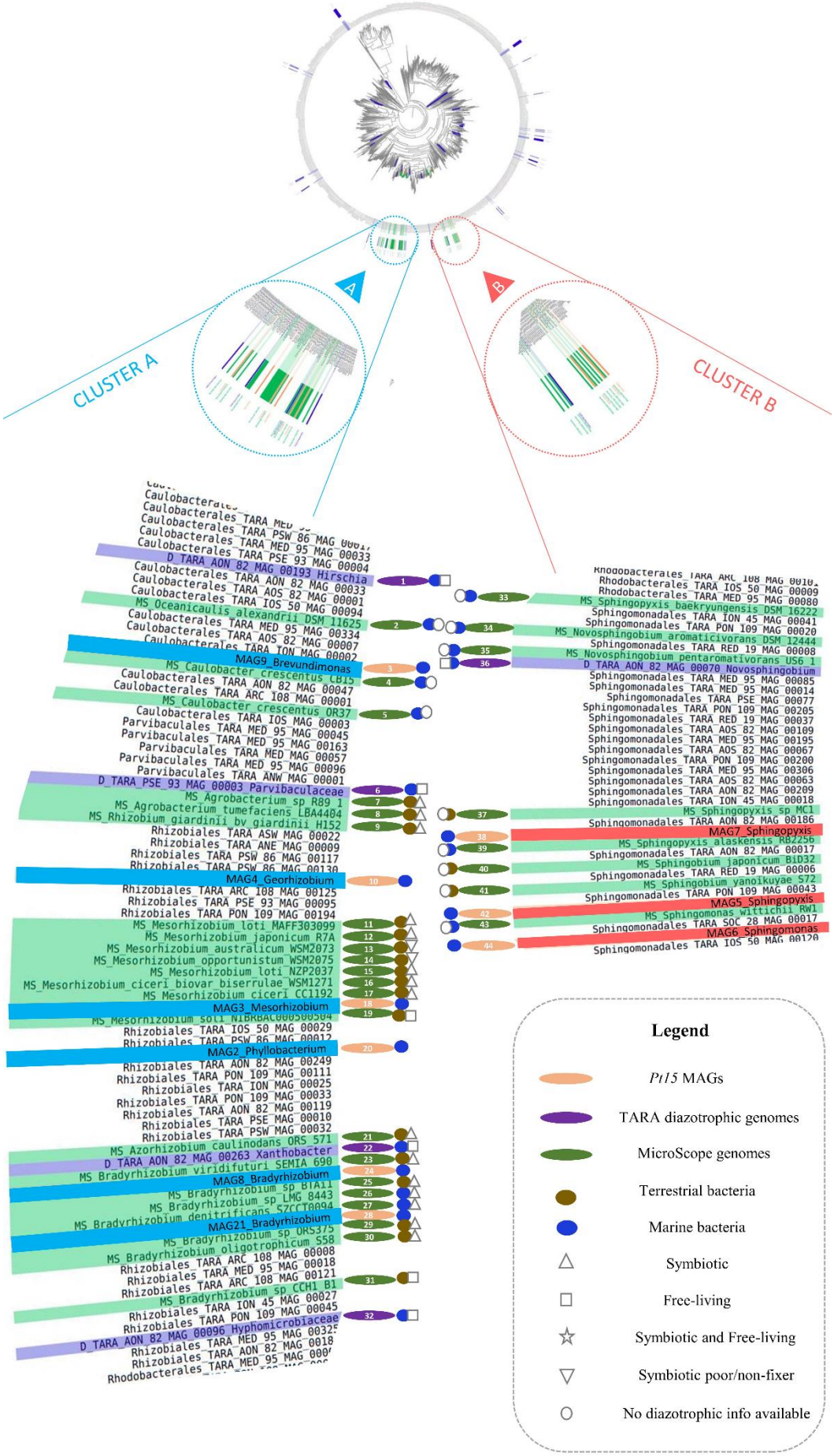
CLUSTER A
CLUSTER B
A
B
Caulobacterales TARA PSW 86 MAG 00033
Caulobacterales TARA MED 95 MAG 00033
Caulobacterales TARA PSE 93 MAG 00004
D_TARA_AON_82_MAG_00193_Hirschia
Caulobacterales TARA AON 82 MAG 00033
Caulobacterales TARA AOS 82 MAG 00001
Caulobacterales TARA IOS 50 MAG 00094
MS_Oceanicaulis_alexandrii_DSM_11625
Caulobacterales TARA MED 95 MAG 00334
Caulobacterales TARA AOS 82 MAG 00007
MAG9_Brevundimonas
MS_Caulobacter_crescentus_CB15
Caulobacterales TARA AON 82 MAG 00047
Caulobacterales TARA ARC 108 MAG 00001
MS_Caulobacter_crescentus_OR37
Caulobacterales TARA IOS MAG 00003
Parvibaculales TARA MED 95 MAG 00045
Parvibaculales TARA MED 95 MAG 00163
Parvibaculales TARA MED MAG 00057
Parvibaculales TARA MED 95 MAG 00096
Parvibaculales TARA ANW MAG 00001
D_TARA_PSE_93_MAG_00003_Parvibaculaceae
MS_Agrobacterium_sp_R89_1
MS_Agrobacterium_tumefaciens_LBA4404
MS_Rhizobium_giardinii_bv_giardinii_H152
Rhizobiales TARA ASW MAG 00022
Rhizobiales TARA ANE MAG 00009
Rhizobiales TARA PSW 86 MAG 00117
MAG4_Georhizobium
Rhizobiales TARA ARC 108 MAG 00125
Rhizobiales TARA PSE 93 MAG 00095
Rhizobiales TARA PON 109 MAG 00194
MS_Mesorhizobium_loti_MAFF303099
MS_Mesorhizobium_japonicum_R7A
MS_Mesorhizobium_australicum_WSM2073
MS_Mesorhizobium_opportunistum_WSM2075
MS_Mesorhizobium_loti_NZP2037
MS_Mesorhizobium_ciceri_biovar_biserrulae_WSM1271
MS_Mesorhizobium_ciceri_CC1192
MAG3_Mesorhizobium
Rhizobiales TARA IOS 50 MAG 00029
MAG2_Phyllobacterium
Rhizobiales TARA AON 82 MAG 00249
Rhizobiales TARA PON 109 MAG 00111
Rhizobiales TARA ION MAG 00025
Rhizobiales TARA PON 109 MAG 00033
Rhizobiales TARA AON 82 MAG 00119
Rhizobiales TARA PSE MAG 00010
Rhizobiales TARA PSW MAG 00032
MS_Azorhizobium_caulinodans_ORS_571
D_TARA_AON_82_MAG_00263_Xanthobacter
MS_Bradyrhizobium_viridifuturi_SEMIA_690
MAG8_Bradyrhizobium
MS_Bradyrhizobium_sp_BTA11
MS_Bradyrhizobium_sp_LMG_8443
MS_Bradyrhizobium_sp_S2CCT0094
MS_Bradyrhizobium_denitrificans_S2CCT0094
MAG21_Bradyrhizobium
MS_Bradyrhizobium_sp_ORS375
MS_Bradyrhizobium_oligotrophicum_S58
MS_Bradyrhizobium_sp_CCH1_B1
Rhizobiales TARA ARC 108 MAG 00008
Rhizobiales TARA MED 95 MAG 00018
Rhizobiales TARA ARC 108 MAG 00121
MS_Bradyrhizobium_sp_CCH1_B1
Rhizobiales TARA ION 45 MAG 00027
Rhizobiales TARA PON 109 MAG 00045
Rhizobiales_hyphomicrobiaceae
D_TARA_AON_82_MAG_00096_Hyphomicrobiaceae
Rhizobiales TARA MED 95 MAG 00018
Rhizobiales TARA AON 82 MAG 00018
Rhizobiales TARA MED 95 MAG 000
Rhodobacterales TARA IOS 50 MAG 00009
Rhodobacterales TARA MED 95 MAG 00080
MS_Sphingopyxis_baekryungensis_DSM_16222
Sphingomonadales TARA ION 45 MAG 00041
Sphingomonadales TARA PON 109 MAG 00020
MS_Novosphingobium_aromaticivorans_DSM_12444
Sphingomonadales TARA RED 19 MAG 00008
MS_Novosphingobium_pentaromativorans_US6_1
D_TARA_AON_82_MAG_00070_Novosphingobium
Sphingomonadales TARA MED 95 MAG 00085
Sphingomonadales TARA MED 95 MAG 00014
Sphingomonadales TARA PSE MAG 00077
Sphingomonadales TARA PON 109 MAG 00205
Sphingomonadales TARA RED 19 MAG 00037
Sphingomonadales TARA AOS 82 MAG 00109
Sphingomonadales TARA MED 95 MAG 00195
Sphingomonadales TARA AOS 82 MAG 00067
Sphingomonadales TARA PON 109 MAG 00200
Sphingomonadales TARA MED 95 MAG 00306
Sphingomonadales TARA AOS 82 MAG 00063
Sphingomonadales TARA AON 82 MAG 00209
Sphingomonadales TARA ION 45 MAG 00018
MS_Sphingopyxis_Sp_MC1
Sphingomonadales TARA AON 82 MAG 00186
MAG7_Sphingopyxis
MS_Sphingopyxis_alaskensis_RB2256
Sphingomonadales TARA AON 82 MAG 00017
MS_Sphingobium_japonicum_BiD32
Sphingomonadales TARA RED 19 MAG 00006
MS_Sphingobium_yanoikuyae_S72
Sphingomonadales TARA PON 109 MAG 00043
MAG5_Sphingopyxis
MS_Sphingomonas_wittichii_RW1
Sphingomonadales TARA SOC 28 MAG 00017
MAG6_Sphingomonas
Sphingomonadales TARA IOS 50 MAG 00120
Legend
Pt15 MAGs
TARA diazotrophic genomes
MicroScope genomes
Terrestrial bacteria
Marine bacteria
Symbiotic
Free-living
Symbiotic and Free-living
Symbiotic poor/non-fixer
No diazotrophic info available

289

Phylogenomic analysis of *Pt15* MAGs, MAGs of known terrestrial and marine diazotrophs from the MicroScope database [28] and MAGs from *Tara* Oceans data using anvi'o [29] was performed. The genomes from MicroScope were selected by individual phylogenetic analysis of each nine *Pt15* MAG deposited on the platform. Thus, the relatedness on the MAGs represented are to diazotrophic marine (purple), non-diazotrophic marine (white), diazotrophic terrestrial (green) and non-diazotrophic terrestrial (green) bacteria. The phylogeny was built using Anvio platform and in built HMM of 71 scgs (single copy core genes), Bacteria_71. The analysis revealed two clusters of *Pt15* MAGs on the phylogeny, cluster A (blue) and cluster B (red) (**Fig. 3**). Cluster A (*Mesorhizobium*, *Bradyrhizobium* MAGs, *Georhizobium*, *Phylobacterium*, and *Brevundimonas*) was affilated to diazotrophs, while, cluster B (2 *Sphingopyxis* MAGs and *Sphingobium*), was related more to denitrifiers. In both clusters, whenever the related MAGs were not identified as diazotrophs (because of the absence of *nifHDK*, likely due to incomplete assembly), they were found to belong to Rhizobiales, Parvibaculales, Caulobacterales and Sphingomonodales, orders known to contain nitrogen fixing species [30-32]. *Sphinopyxis* MAG5 was identified with *nifH* gene *in silico* and was found to cluster with non- or un-identified diazotrophs. For a clearer depiction of Figure 3, an interactive phylogenetic tree is available on the following link: https://ncdstree.univ-nantes.fr. Altogether, our results including (i) survival of the xenic diatom in the absence of usable forms of nitrogen, (ii) nitrogen fixation demonstrated by ARA and ^{15}N-incorporation, (iii) detection of *nifH*, and (iv) the isolation of NCDs from the xenic *Pt15* clustering with known proteobacteria diazotrophs namely rhizobia, indicate that an interaction for nitrogen fixation likely occurs in *Pt15* xenic cultures, supporting the survival of diatoms in -N condition.

Functional gene annotation of *Pt15* associated NCDs in nitrate deplete versus replete conditions

To understand the biological functions of the microbial community, genes from -N and +N treatments were assigned to functional categories (**Fig. 4, Table S4**). There was a significant enrichment of genes related to nitrogen fixation and metabolism in -N compared to +N condition. Typically, in -N, we exclusively identified *nifH* and *nifD*, two key components of the nitrogenase enzyme complex. Likewise, *nifX* and *nifT* were only detected in -N suggesting their critical role in nitrogen fixation. Part of the *nif* operon, *NifX* was reported to be important in FeMo-co maturation and its transfer to *NifDK* proteins [33, 34]. Other genes related to nitrogen fixation metabolism emerged from the analysis, namely *HemN*, *Fpr*, *FixS*, *FixA*, *FixH*, *GroEL*, *NifS* and *FixJ* (**Fig. 4**), some of which are part of the NIF regulon.

The abundance of several transporters was striking in -N, suggesting an important role in energy/substrate shuttling between the host and the bacterial community. Examples included an *EcfT* gene (energy-coupling factor transporter transmembrane) known for its function in providing the energy necessary to transport a number of different substrates [35], AcpS, an acyl carrier gene, which functions as a multi-carbon units carrier into different biosynthetic pathways [36], TauB, a taurine transporter that might play a role in providing taurine, which is produced by a large number of algae and known as a potential source of carbon, nitrogen and energy [37].

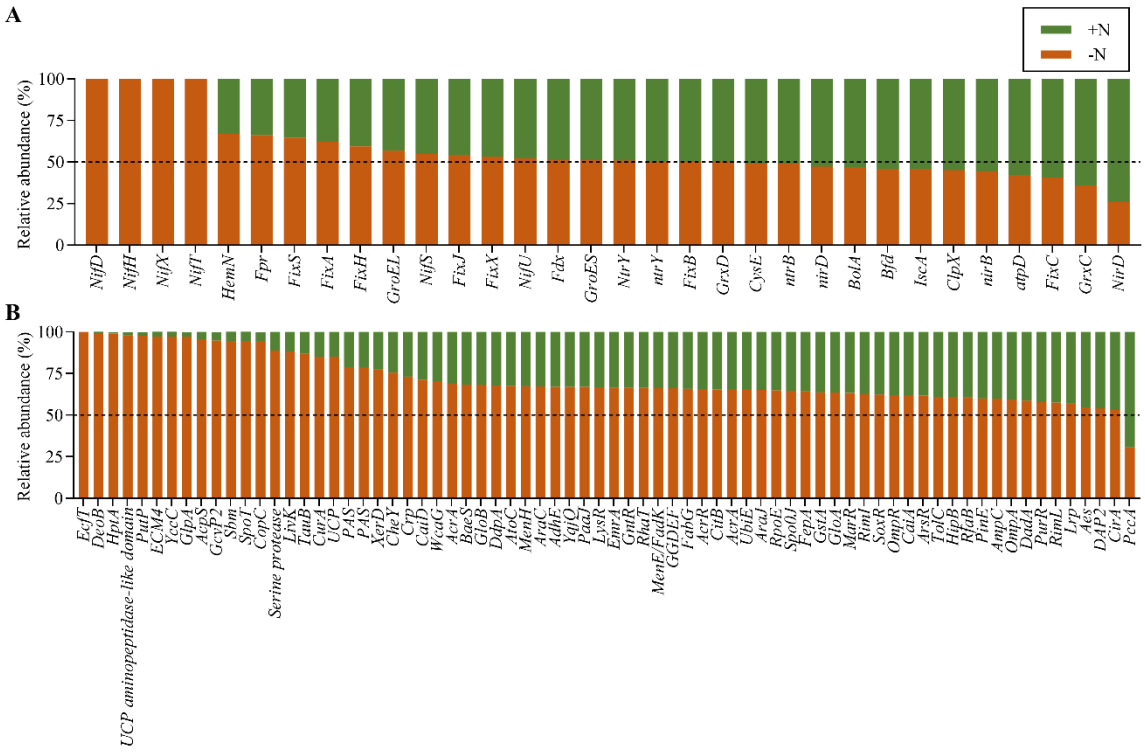

Fig. 4. Functional gene annotation of *Pt15* associated NCDs in nitrate deplete versus replete conditions

A, Relative abundance of selected genes involved in nitrogen fixation and assimilation in nitrate deplete and nitrate replete conditions. B**,** illustration representing a combined view of 50 top abundant gene in nitrate deplete and replete condition with ordering representing top relatively abundant genes in nitrate deplete conditions. Dashed line indicates the relative percentage at 50%.

Stress responsive genes were clearly more represented in -N compared to +N including SpoT, which is a general bacterial stress response [38] that allows bacteria to increase its persistence in stressful conditions, here the lack of nitrogen. Other genes found almost exclusively in the starved bacterial community were the PAS domain containing genes (Per-ARNT-Sim) [39],

which function as signal sensors by their capacity to bind small molecules, modulators and transducers. They are known to sense oxygen to prevent degradation of oxygen sensitive enzymes suggesting a crucial and protective role in -N condition where there is an enrichment in nitrogenase containing bacteria. Overall, functional analysis of MetaG data corroborated with NCDs enrichment in -N and nitrogen fixation.

Geographical distribution and ecological prevalence of NCD-microalgae interactions

Next, we sought to assess the prevalence and importance of similar interactions in other microalgae providing further evidence that the association of NCDs with *P. tricornutum* is not an isolated case. First, we screened a collection of 14 xenic microalgae as described for *Pt15,* and identified five species of microalgae (35%) that grew in the absence of nitrogen in the growth medium suggesting the presence of diazotrophs (**Table S5**). Similar to *Pt15*, the retained microalgae were screened using different nitrogen deprived media under various conditions for diazotrophs isolation. *NifH* degenerate and 16S rRNA gene primers were used to identify the isolated bacterial colonies, which revealed five Alpha-proteobacteria including two species of *Thalassiospira sp*. (isolated from two different microalgae), *Stenotrophomonas maltophilia*, *Stappia* and *Rhodococcus qingshengii* suggesting that the occurrence of NCDs with microalgae may be relatively common. PCR detection using *nifH* degenerate primers was successful only in *S. maltophilia*. In all other bacteria, with the exception of *Stappia* and *S. maltophilia* which were not tested, a reduction of acetylene to ethylene was observed in the ARA assay **(Table S5)**. All isolated bacterial species grew in nitrogen free medium (**Table S5**). To provide additional support for the presence of nitrogen fixation in bacteria isolated from microalgae other than *P. tricornutum*, we carried out an $^{15}N_2$ incorporation assay followed by LC-MS analysis on *Rhodococcus.* The results clearly indicated that the bacteria assimilated labeled nitrogen, confirming its ability to fix nitrogen (**Table S1**).

To maximize the number of species sequenced while maintaining cost-effectiveness, isolated NCDs were sequenced in pools of three bacteria using both Illumina and PacBio. Their genomes were successfully assembled, demonstrating high completeness (>87%, with two MAGs reaching 100%) and low contamination (**Table S3**). We then used MAGs isolated from *Pt15* and the other microalgae (**Table 1 and Table S3**) to reassess their phylogenetic relationship as described for *Pt15* isolated NCDs. The analysis revealed 3 more clusters (C, D and E) in close proximity to diazotrophic MAGs from the environment and/or MAGs belonging

to diazotrophic containing orders [40] [41] [42] (**Figure S3**). An interactive figure is available at https://ncdstree2.univ-nantes.fr/.

Next, we assessed the occurrence of *Pt15* MAGs in the environment in surface water and Deep Chlorophyll Maximum layer (DCM) using *Tara* Ocean datasets [43, 44]. Given that *Pt15* MAGs had not been previously reported, the analysis to monitor the distribution for the surface and DCM waters was performed using the two phylogenetically closest TARA MAGs. The phylogeny was built in Anvio with 1888 TARA MAGs with inbuilt single copy genes HMM (Bacteria_71) and the five *Pt15* MAGs in which the *nifH* gene was identified. We used branch support and branch length as proxies to select the closely related TARA MAGS. The two TARA MAGs clustering with each individual *Pt15* MAG were selected (**Table S3**). With the exception of two *Pt15* MAGs, *Georhizobium* and *Sphingomonas*, which show weak branch support with one of the two TARA MAGs, all other MAGs are robustly supported as being closely related to their respective TARA MAGs in the phylogeny. Among the 130 sampling stations, 92 stations showed the occurrence of at least one of the TARA affiliated MAGs reflecting a high prevalence (**Fig. 5A, Figure S4**). *Pt15* clustering with *Tara* MAGs were more frequently occurring with 129 recorded stations. The distribution of these MAGs was extensive, spanning all latitudes from south Pacific, Indian and Atlantic Oceans to polar regions. The MAGs were found in both surface and DCM samples, mainly within the 0.8-5µm and 0.22-1.6/3µm size fractions (**Fig. 5A, Figure S4**). Interestingly, TARA MAGs affiliated to *Pt15* MAGs co-occurred in surface and DCM samples in most cases, although their dominance in surface samples was prominent (**Fig. 5B**).

Fig. 5. Geographical distribution and ecological prevalence of isolated and assembled bacterial diazotrophs genomes correlating to TARA data

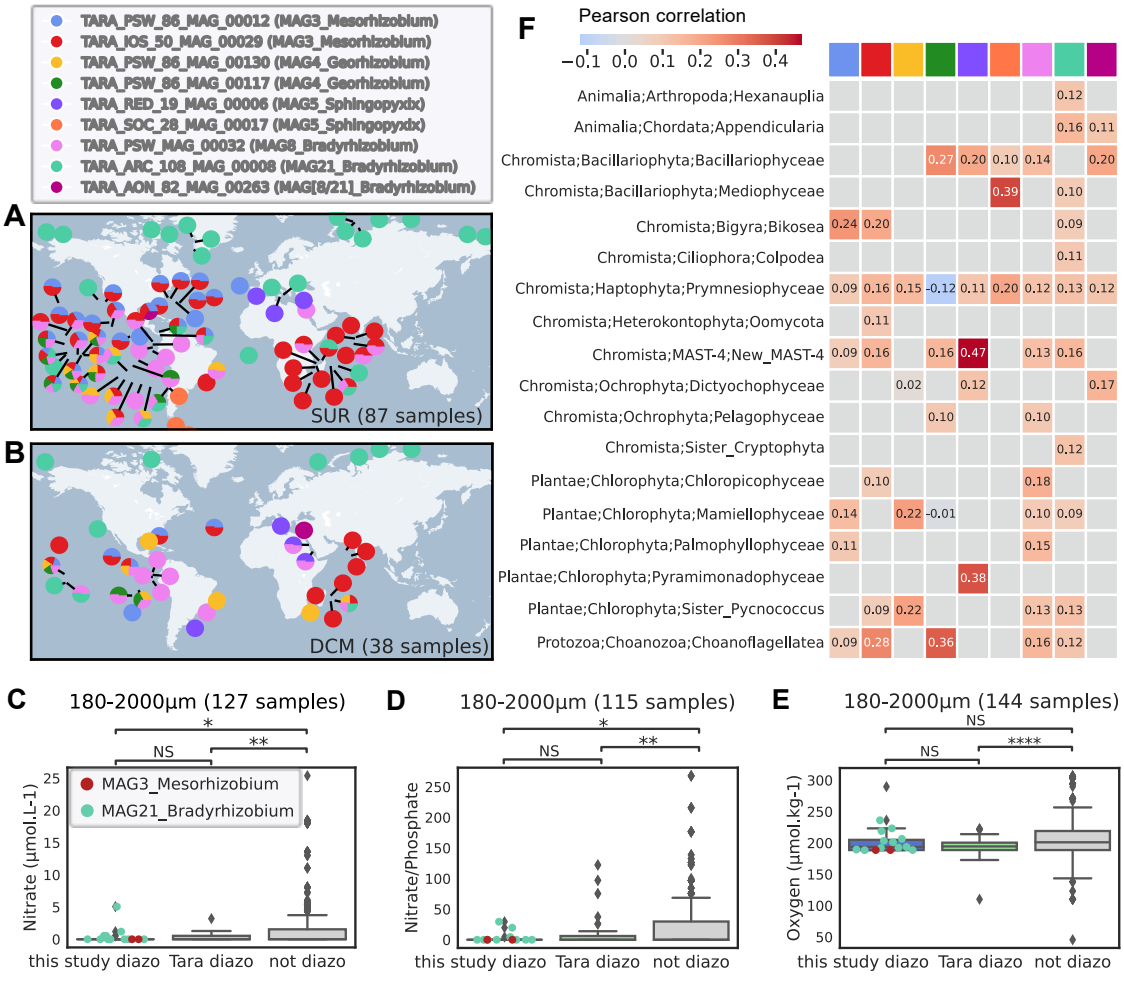

Geographical distribution of phylogenetically closest *Pt15* associated TARA ocean MAGs in A, surface and B, DCM samples. C-E, relative abundance of the top 2 most occurring MAGs of *Pt15* bacterial community in the environment in function of (C, nitrate, D, N/P ratio and E, oxygen concentration). F, Co-occurrence of TARA MAGs affiliated to *Pt15* in the environment with different species of micro-eukaryotes inferred through FlashWeave, FDR <0.01.

We then asked whether the occurrence of the MAGs isolated from *Pt15* correlated with environmental factors monitored during the *Tara* Oceans campaign and whether they co-occur with other organisms. We considered only two *Pt15* MAGs (*Mesorhizobium* MAG3 and *Bradyrhizobium* MAG21) to assess their correlation with three environmental factors used as indicators of diazotrophy, namely nitrate, nitrate phosphate ratio and oxygen concentrations. Iron concentrations from the ECCO2-DARWIN model [45] were considered, yet no distinct relationship was identified with the distribution of NCDs. Interestingly, TARA affiliated MAGs were detected in low nitrate and almost no detection above 5 µM (**Fig. 5C**). For both nitrate and N/P ratio, there are no differences in their occurrence with TARA diazotrophic MAGs,

while these differences are significant with non-diazotrophic MAGs only in the larger size fraction of 180-2000 µm (**Fig. 5C and D**) suggesting an association with particles, aggregates or other organisms. This measure is in line with nitrate limitation as a marker of diazotrophs presence [46]. In a similar way, oxygen showed a consistent pattern when comparing this study's MAGs with TARA NCDs, distinguishing these two categories from non-diazotrophic MAGs only in 0.22-1.6/3 µm, 0.8-5 µm and 180-2000 µm size fractions (**Fig. 5E and Figure S5**). By contrast to what is known about oxygen inhibition of nitrogenase, both MAGs seemed to thrive in relatively well oxygenated zones (200 µM) compared to less oxygenated areas or oxygen minimum zones (OMZ, 20- 50 µM O_2). This implies adaptive means by which these bacteria fix nitrogen such as creating micro-oxic environments through their interactions with other organisms.

Strikingly, a co-occurrence analysis revealed a clear association of the NCDs isolated from *Pt15* (**Fig 5H**) with micro-eukaryotes. Most of the *Pt15*-associated TARA MAGs were found to co-occur primarily with Haptophytes, Bacillariophyta, and Cryptophytes. The association with Bacillariophyta is consistent with their isolation from a diatom. While we did not demonstrate nitrogen fixation in these predicted associations, this analysis provides evidence for a probable nitrogen fixing interaction between *Pt15* MAGs and various species of primarily photosynthetic micro-eukaryotes.

Discussion

Recent reports of NCDs dominance in the euphotic zones of the oceans questioned the long-held dogma that symbiotic N_2 fixation is mainly carried by cyanobacteria, but also raised fundamental questions on how these presumably heterotroph NCDs can thrive in the sunlit ocean [12-14, 47]. The nitrogenase enzyme complex responsible for nitrogen fixation is sensitive to oxygen that irreversibly inactivates the enzyme. Therefore, diazotrophs evolved several mechanisms to protect nitrogenase from oxygen degradation including hyper-respiration, uncoupling of photosynthesis in space and time in photosynthetic diazotrophs, and attachment/interaction with microalgae or debris which were found to be hotspots of nitrogen fixation [17]. Using a multidisciplinary approach, the study described herein brings evidence of interactions for nitrogen fixation between microalgae, in particular the model diatom *Phaeodactylum tricornutum* and NCDs. After screening ten xenic accessions of *P. tricornutum* in the absence of a usable form of nitrogen, our study revealed that one accession, *Pt15*, interacts

with nitrogen-fixing proteobacteria. Although low, this nitrogen fixation and uptake seemed to maintain the viability of the diatom and its associated bacteria. To compensate for the allocation of energy to the bacterial community, *Pt15* cells seemed to slow down growth. This diatom-NCDs interaction may reflect natural environments, where such interactions, in extreme conditions (low to no nitrogen) take place until favorable factors (e.g., nitrate repletion with upwelling or Sahara dust) permit the recovery and growth of cells, such as what we observed in our nitrate starved cultures when transferred to nitrate replete medium.

Metagenomic sequencing of the associated bacteria revealed not only one diazotrophic species but a group of nitrogen fixers predominantly Alpha-proteobacteria, mainly represented by Rhizobiaceae, Sphingomonadaceae and Xanthobacteraceae. All the isolated bacteria identified as diazotrophs grew in nitrogen free medium. The nitrogenase gene was detected in the majority of them, through either in silico analysis or by PCR amplification, further confirming the presence of diazotrophy in these bacteria. The *nifH* gene was found in most cases in the chromosome, except for *Georhizobium* where it was predicted to be plasmidic. ARA results indicated that nitrogen fixation rates in xenic *Pt15* under -N condition were lower than those observed in the positive controls and showed variability when compared to nitrogen fixation rates reported for NCDs in natural environments. These differences likely reflect the variability in environmental conditions across study sites. For example, in the Gotland Basin, NCD nitrogen fixation rates were estimated at approximately 7.6 nmol/L/day in surface waters and 0.44 nmol/L/day in deep waters [48]. In contrast, nitrogen fixation rates of NCDs in hypoxic waters of the Southern Californian Bight averaged 0.07 nmol/L/day, which is lower than those observed in the present study [49]. However, differences in monitoring techniques and experimental conditions, particularly between in situ measurements and laboratory cultures, must be considered when drawing comparisons [48-51]. The low nitrogen fixation rates observed in xenic *Pt15* and its associated bacterial community under nitrogen-depleted conditions are likely due to competition for fixed nitrogen by non-diazotrophic bacterial species. Another contributing factor may be the quiescent state of diatom cells induced by the absence of nitrogen in the culture. Our data indicate that diatom cells ceased division and likely maintained only minimal metabolic activity, which could have reduced the availability of photosynthates for associated bacteria. Quiescence is a well-documented survival strategy in certain microalgae under unfavorable environmental conditions, allowing them to save energy and sustain basic cellular functions until nutrient availability improves [52-54]. This was evident in *Pt15* cells, which resumed growth upon transfer to nitrogen-rich medium. If *Pt15* is

not in an optimal physiological state to supply energy to its associated bacteria, nitrogen fixation rates will remain low, further exacerbated by the consumption of fixed nitrogen by the abundant non-diazotrophic bacteria present in the culture.

The nitrogen-fixing capability of the isolated bacteria was directly confirmed using $^{15}N_2$ incorporation monitored by isotope analysis in LC-MS, leaving no doubt about the *Pt15* associated bacteria's ability to fix nitrogen. This provides initial evidence that NCDs associated with the diatom are capable of fixing nitrogen, a process likely beneficial to other associated bacteria and potentially to the diatom, as long as it does not transition into a resting stage due to the extreme culture conditions, specifically the complete absence of bioavailable nitrogen. A recent study identified an NCD from the Rhizobiales order residing within a diatom of the *Halsea* genus, functioning as an endosymbiont [20]. The interactions we identified differ significantly from those with *Haslea* containing NCDs. The bacteria associated with *Haslea* have a much smaller genome, typically less than 1 Mb, whereas our NCDs have genomes about 7 Mb in size [20]. This discrepancy in genome size reflects the different types of interactions: in the obligate interaction, the bacteria have lost parts of their genome and depend on the host's cellular machinery, whereas in the facultative interaction, the bacteria interact from a distance or within the phycosphere [55-58]. Our findings reflect the broad array of nitrogen fixation interactions, extending from obligatory symbiosis to epibiosis or remote interactions within the phycosphere, mirroring observations in nitrogen fixing interactions between Rhizobia and land plants. Bacteria associated with *Pt15*, identified as NCDs in this study, align with the distribution patterns of *Tara* NCDs in ocean regions characterized by low nitrate and nitrate phosphate ratio. Interestingly, their distribution and correlation with these environmental factors are observed only in larger size fractions. This observation is in accordance with findings from multiple studies that have reported similar diazotroph distributions under the aforementioned conditions. Indeed, diazotrophs have developed various strategies to counteract the irreversible degradation of the nitrogenase enzyme by oxygen [6, 7, 10, 59]. These strategies include forming associations with other organisms, among other mechanisms, as they seek out low-oxygen environments primarily facilitated by surrounding polymers.

Our study revealed that NCDs interaction with *Pt15* and other microalgae is likely not an isolated phenomenon and is more broadly distributed than previously anticipated. Our MAGs were detected in the environment clustering with previously identified terrestrial and marine NCDs, supporting diazotrophy and likely their ecological importance. These MAGs were identified at global scale in surface and DCM samples in size fractions enriched in microalgae,

which supports the hypothesis of an interaction with them as evidenced by the co-occurrence analysis. This interaction might be taking advantage of hypo-oxic biomes microalgae and bacteria may provide with the secretion of extracellular polymers, mainly polysaccharides, that form biofilms ensuring low O_2 diffusion [60-62]. This was suggested by our TEM analysis with the formation of pellicles around *Pt* cells and bacteria. Such pellicles were reported to form around two nitrogen fixing bacteria, *P. stutzeri* and *Azospirillum brasilense* in oxygenated surroundings implying the importance of oxygen stress in the formation of these structures [63]. The presence of these sac-like structures might have hindered diatom uptake of released ammonium leading to growth inhibition in the extreme condition tested in this study. Besides biofilm formation, this interaction may combine different strategies for both microalgae and NCDs to avoid/limit oxygen inactivation of nitrogenase such as a conformational switch that protects nitrogenase from O_2 degradation [10, 64] or hyper-respiration [65] among other protective mechanisms that need further investigations. In line with our discovery of NCDs interaction with microalgae for nitrogen fixation, a recent study [66] suggested that anaerobic processes, including heterotrophic N_2 fixation, can take place in anoxic microenvironments inside sinking particles even in fully oxygenated marine waters.

Conclusions

Our screen under nitrogen-deprived conditions of different accessions of the model diatom *P. tricornutum* revealed several previously unidentified NCDs among which some were found to be related to terrestrial nitrogen-fixing bacteria, raising questions about their evolutionary origins. The NCDs associated with *P. tricornutum* enable the diatom to survive in nitrogen-deprived environments, indicating a relationship that supports its persistence. These NCDs remain in the phycosphere and do not penetrate diatom cells, suggesting that their interactions occur at a distance. Genome analyses of *P. tricornutum*-associated bacteria showed clustering with both terrestrial and marine NCDs, and these bacteria were found to be widely distributed across latitudes, co-occurring with photosynthetic microeukaryotes, including diatoms, haptophytes, and cryptophytes. The identification of different NCDs with a model diatom opens wide perspectives to investigate the role of individual and combined interactions of bacterial species with the host and within the bacterial community. Thus, *Pt15* accession with its associated NCDs represent a unique Eukaryotic-bacteria model system and an exciting opportunity to study molecular mechanisms underlying this interaction for nitrogen fixation and beyond.

Methods

Microalgae species used and culture media

Screening of Phaeodactylum tricornutum accessions

Eleven xenic *P. tricornutum* accessions were screened in presence (545 µM) and absence of nitrate in Enhanced Artificial Sea Water (EASW) in order to select xenic *Pt* ecotype growing in the absence of nitrate. The starting concentration for all accessions, measured under the microscope using Malassez counting chamber, was 100,000 cells per ml. The cells were counted and washed twice with nitrate-free EASW in order to remove all residual nitrate and resuspended in respective media for screening over a period of one month. A growth curve was made by counting the cells in periodic time intervals. The cultures were grown at 19°C with a 12/12 hours photoperiod at 30 to 50 µE/s/m2. A cocktail of antibiotics (Ampicillin 100 µg/µl, Chloramphenicol (14 µg/µl) and Streptomycin 100 µg/µl) was used to make *Pt15* axenic in liquid EASW culture medium with refreshment of antibiotic containing medium every 5 days. *Pt15* cells were regularly monitored for axenicity using peptone-rich medium and microscopy. Additionally, axenicity was further validated by culturing the putatively axenic *Pt15* in -N medium. If the *Pt15* cells died under these conditions, it would confirm the absence of associated bacteria.

Screening of other microalgae

A total of fourteen microalgae were screened in nitrate-deplete and nitrate-replete enhanced artificial sea water for growth (Table S5). About 100,000 cells were counted, resuspended in their respective media and grown as described above. Their growth was assessed for a period of two weeks at regular intervals.

Acetylene reduction assay

Acetylene reduction assay (ARA) [21] was used to quantify the conversion of acetylene to ethylene (C_2H_4) which allows the assessment of nitrogenase activity. ARA was conducted on the following samples: two positive controls, *Azotobacter. vinelandii* (NCIMB 12096), *Pseudomonas stutzeri* BAL361, xenic *Pt15* grown in NFM [67, 68] or nitrogen replete medium, all incubated at three different temperatures (19, 25, 30°C). Axenic *Pt15* culture grown in NFM medium + 5 sugars (final concentration of 1% each: D-glucose, D-sucrose, D-fructose, D-galactose and D-mannose) was used in every measurement as a negative control to ensure there was no endogenous ethylene produced. All the cultures were grown at their respective growth media and conditions. After reaching an appropriate O.D. between 0.2-0.3, 1 ml of the bacterial cells were collected in an Eppendorf's tube and centrifuged at11,000 rpm for 10 minutes at RT

to remove the medium. The cells were re-suspended in NFM with five sugars and grown in their respective medium. Sugar was not used for culturing xenic *Pt15*. When the bacterial growth reached an O.D. of 0.2-0.3, the cultures were prepared for acetylene reduction assay. The cultures were secured with a rubber stopper in order to make them air tight. Ten percent of the air was removed from the culture flasks and supplemented with 10% acetylene gas. The cultures were incubated at their appropriate temperatures for a period of 72 hours before monitoring ARA with gas chromatography. A volume of 500 µl was taken from the headspace of the samples using a Hamilton gas tight syringe (SYR 500 ul 750 RN no NDL, NDL large RN 6/pk) and injected into an Agilent gas chromatograph model 7820 model equipped with a Flame Ionization Detector (GC-FID) and using Hydrogen as carrier gas at a constant flow of 7.7 mL/min. Samples were injected into a split/splitless injector, set at 160℃ in splitless mode. A GS-Alumina capillary column, 50 m × 0.53 mm × 0.25 µm (Agilent, 115-3552) was used. The programmed oven temperature was at 160℃ (isotherm program) during 2 min. The FID detector was set to 160℃. A standard curve was made with ethylene gas using 5 volumes (100, 150, 200 µl). The raw data generated from the GC provides value of y, Area [pA*s]. This value is supplemented in the slope-intercept formula, y = mx + c, with 'm' and 'c' representing slope and constant values respectively, denoted in the calibration curve. The amounts of ethylene were calculated as described previously [69]. Acetylene reduction rates were converted to fixed N using the common 3:1 (C2H2 :N2) molar conversion ratio [70, 71].

Particulate organic nitrogen measurements

One liter of 200,000 cells/ml culture of xenic *Pt15* was grown in nitrate-free EASW for over a period of 80-days at 19°C and 12h/12h light/dark photo period at 70µE/s/m2. Six time points were used for harvesting samples: 1, 4, 12, 59, 76 and 80 day(s). The cells were counted at each time point using a cell counter. Twenty ml of *Pt15* culture were harvested and injected through a sterile (treated at 450 deg/4hrs) Whatman GF/F glass microfibre filter paper to collect *Pt15* cells and the filters were dried overnight in 60°C incubator and stored at -80°C. The 20 ml filtrate from the cultures was passed through 0.22 µm filters (Sigma ca. GVWP10050), in order to remove bacterial cells and stored at -80°C, before being processed for particulate organic nitrogen measurement analysis. EASW with 545 µM nitrate, 0 µM nitrate and three heat-treated Whatman GF/F glass microfibre filters were used as blanks for comparison with test samples.

Test for incorporation of the ^{15}N isotope

Stationary cultures (30 mL) of either the diatoms, *Phaeodactylum tricornutum Pt15* Xenic Plus nitrate (545 µM), *P. tricornutum Pt15* Xenic Minus nitrate (0 µM), *P. tricornutum Pt15* Axenic Plus nitrate (545 µM) or bacteria, *Bradyrhizobium MAG21*, *Methylobacterium*, *Azotobacter vinalendii*, *Pseudomonas stutzeri BAL361*, *Escherichia coli DH5a* and *Rhodococcus* were put under a $^{15}N_2$-(98 atom %, Sigma-Aldrich, Steinheim, Germany) atmosphere (20 mL). For this, a 50 mL syringe (B Braun Omnifix®) without needle was used to take up 30 mL of the culture, followed by 20 mL of 15N2 from a lecture bottle. The syringes were immediately sealed with a plastic valve and parafilm to prevent leakage of the gas. Diatom cultures were incubated at 18 °C under a 14:10 h light: dark regime with an illumination of 60-65 µmol photons m^{-2} s^{-1}. Bacterial cultures were incubated at 100 rpm and 30 °C, except for *E. coli DH5a* which was incubated at 37 °C. After 2.5 days the diatom cultures were filtered (1.2 µm pore size, GF/C, Whatman, GE Healthcare, Little Chalfont, United Kingdom). The cells were washed off the filter using 5 mL ice-cold methanol/ethanol/chloroform 1:3:1 (methanol: HiPerSolv Chromanorm, VWR Chemicals, Dresden, Germany; ethanol: HiPerSolv Chromanorm, VWR Chemicals, Dresden, Germany; chloroform: SupraSolv, VWR Chemicals, Dresden, Germany) and the resulting extracts were treated in an ultrasonic bath for 10 min and centrifuged (16.100 x g, 20 min, 4 °C). The supernatant was stored at -20 °C until analysis. Bacterial cultures were centrifuged (3.893 x g, 20 min, 4 °C) and the cells were resuspended in 5 mL of methanol/dichlormethane/ethylacetate 10:2:3 (dichlormethane: SupraSolv, VWR Chemicals, Dresden, Germany; ethylacetate, HiPerSolv Chromanorm, VWR Chemicals, Dresden, Germany). The suspensions were sonicated (5 min, 9 cycles, 80-85 %) and afterwards centrifuged (3893 x g, 20 min, 4 °C). The supernatant was stored at -20 °C until further use.

Test for uptake of ^{15}N-L-valine-by *P. tricornutum*

To stationary cultures (40 mL) of either *Phaeodactylum tricornutum Pt15* Xenic Plus nitrate (545 µM) or *P. tricornutum Pt15* Xenic Minus nitrate (0 µM), 100 µL of an aqueous ^{15}N-L-valine- solution (98 atom % ^{15}N, Merck, Saint Louis, USA, 50 µmol L^{-1} in medium) were added to reach a final concentration of 125 nm L^{-1}. The cultures were then incubated, extracted and the samples stored as described in "*Test for incorporation of the ^{15}N isotope".*

Analysis of endometabolomes with LC-MS

Cell extracts were dried in a nitrogen stream at room temperature and resuspended in either 200 µL methanol for diatom extracts or methanol/acetonitrile/water 5:9:1 (acetonitrile:

HiPerSolv Chromanorm, VWR Chemicals, Dresden, Germany; water: CHEMSOLUTE, TH.GEYER, Renningen, Germany) for bacterial extracts. Metabolites were separated on a Dionex Ultimate 3000 UHPLC coupled to a Q-Exactive Plus Orbitrap mass spectrometer (Thermo Scientific, Bremen, Germany). Chromatographic separation was performed on a SeQuant ZIC-HILIC column (5 µm, 200 Å, 150 × 2.1 mm, Merck, Germany) equipped with a SeQuant ZIC-HILIC guard column (20 × 2.1 mm, Merck, Germany) at 25 °C using water with 2 % acetonitrile and 0.1 % formic acid as eluent A and 90 % acetonitrile with 10 % water and 1 mmol L^{-1} ammonium acetate as eluent B. Full scan measurements (*m/z* 80-1200, resolution 70k, automatic gain control target $3E^6$, maximum ion injection time 200 ms) were performed in positive and negative ion mode using a heated electrospray ionization source to generate molecular ions. The method duration was 14.5 min with an MS runtime from 0.5 min to 9.0 min, a flow rate of 0.6 mL min^{-1} and a gradient as follows: 85 % B (0.0-4.0 min), linear gradient to 100 % A (4.0-5.0 min), 100 % A (5.0-9.0 min), linear gradient to 100 % B (9.0-10.0 min), 100 % B (10.0-12.0 min), linear gradient to 85 % B (12.0-12.5 min), 85 % B (12.5-14.5 min). Amino acid standards were run separately for comparison of retention time and mass spectra. Resulting raw data was analyzed with FreeStyle (Thermo Fisher Scientific).

Microscopy

Light microscopy

Living cells grown on agar plates were used directly for the preparations. Cells were taken directly from agar plates without prior treatment, transferred onto glass slides, and covered with a cover slip before observation. Samples were observed with differential interference contrast (DIC) microscopy by BX53 microscope (Olympus, Japan) and Axiocam 705 color (Carl Zeiss, Germany).

Transmission electron microscopy

Samples were prepared as described previously [72]. Embedded samples were cut for making pale yellow ultra-thin sections (70-80nm thickness) with a microtome EM UC6 (Leica Microsystems, Germany). Sections were stained with TI blue (Nisshin EM, Japan) and lead citrate for inspection with an electron microscope JEM-1011KM II (JEOL, Japan).

Bacterial isolation and culture media used

A total of eight media recipes were used for bacteria isolation and culture under different conditions, all summarized in Supplementary File 1. All isolated bacteria were checked for purity by repeated streaking and 16S sequencing. Bacterial species were maintained in 20% glycerol at - 80°C for long-term storage.

DNA extraction and PCR amplification of marker genes

For initial identification of bacteria, the isolated colonies were picked under sterile conditions using filter tips, resuspended and mixed thoroughly in 50 µl nuclease-free water (NFW). The suspension was heat/cold treated at 95°C following 4°C, 10 min each and twice for cell lysis. Post-treatment, an additional 50 µl NFW was added to the suspension for a total volume of 100 µl. Five µl of the colony DNA was used as template for PCR.

Wizard® Promega Genomic DNA extraction kit was used for extracting high-quality genomic DNA from bacterial cells. The bacteria were grown in their appropriate media until the culture optical density (OD) reached 0.3. The cells were harvested and washed in 1X PBS twice. The cell pellets were resuspended in 480 µl 50 mM EDTA and treated with 120 µl of 20 mg/ml lyzozyme (VWR cat no. 0663-5G), incubated at 37°C for 60 min in order to lyze possible gram-positive bacteria. Post incubation, the cells were centrifuged and the supernatant was removed. Nuclear Lysis solution, 600 µl (Promega cat no. A7941), was used to re-suspend and gently mix the pellet for incubation at 80°C for 5 min. The suspension was allowed to cool at room temperature (RT) for 10 min before adding 1 µl RNAse at 10 mg/ml (VWR cat no. 0675-250MG) and incubation at 37 for 60 min. After incubation, the suspension was cooled at RT for 10 min. Protein lysis solution, 200 µl (cat no. VWR 0663-5G) was added, vortexed and incubated on ice (4°C for 5 min). The mixture was centrifuged and the clear supernatant was transferred to a clean Eppendorf with 600 µl RT isopropanol and the tube was mixed gently before being centrifuged. The cell pellet was washed with freshly prepared 70% ethanol and re-centrifuged. The ethanol was carefully removed without disturbing the pellet and air dried before resuspension in appropriate amount of NFW. The quality of the DNA was checked using Nanodrop 260/280 and 230/260 ratios and on 1% agarose gel. The identity of the bacteria was re-confirmed using 16S rRNA gene amplification and Sanger sequencing.

For the *nifH* PCR amplification, the reaction mixture included 2.5 µL of DreamTaq Green Buffer (1X), 0.1 µL of BSA (0.08 µg/µL), 2 µL of each primer (10 µM), 0.2 µL of DreamTaq Green Polymerase (5 U/µL), 0.5 µL of dNTP mix (10 mM), 3 µL of DNA template (normalized to 10 ng/µL), and H2O adjusted to a total volume of 25 µL. The thermocycling protocol started

with an initial denaturation step at 95°C for 5 minutes, followed by 40 cycles of denaturation at 95°C for 30 seconds, annealing at 53°C for 30 seconds, and extension at 72°C for 30 seconds, and a final extension step at 72°C for 7 minutes. Following the reaction, amplification results were assessed through 1% agarose gel electrophoresis, and DNA bands of interest were isolated using the NucleoSpin® Gel & PCR Cleanup Kit from Macherey-Nagel. The extracted DNA underwent Sanger sequencing at Eurofins Scientific. Sequences were analyzed using Geneious. For species identification, 16S PCR fd1-rd1, variable regions PCR V1V2 V3V4 and V5V7 were used. The reaction was performed with 35 cycles of 95 °C (1 min), 55 °C (1 min) and 72 °C (1 min). All primer sequence details are reported in supplementary Table 7.

Sample preparation and DNA extraction for Illumina and PacBio sequencing

Duplicate with a starting concentration of 200,000 cells/ml of 3-liter culture volumes of xenic *Pt15* in nitrate-replete and nitrate-deplete enhanced artificial sea water were grown for a period of 2 months (60-days) at 19°C and 12h/12h light/dark photoperiod at 70µE/s/m2 before collection for sequencing. The xenic *Pt15* cells were filtered through a 3 µm filter (MF-millipore hydrophobic nitrocellulose, diameter 47 mm (cat no. SSWP04700) to retain the cells and allow passage of the filtrate containing the bacterial community. The filtrate was filtered twice in order to avoid contamination of the bacterial cells with residual *Pt15* cells. The double filtered bacterial community was collected in 0.22-micron filter (MF-millipore hydrophobic nitrocellulose, diameter 47 mm (cat no. GSWP04700) and resuspended in 1X PBS. DNA was extracted for metagenome sequencing using Quick-DNA fungal/bacterial mini prep kit (cat no. DG005) and according to manufacturer instructions. The bacterial DNA quality was checked using 1% agarose gel to assess intact DNA and quantified using Qubit broad range DNA kit, before being sequenced. Additionally, 16S rRNA sequencing was performed to assess the presence of bacterial DNA and 18S rRNA PCR was run as a negative control to inspect absence of *P. tricornutum* DNA. When bacterial isolates were available, they were sequenced either as a single species or in a pool of 3 bacteria using Illumina and PacBio.

Data processing

Metagenomic analysis

Two different strategies were used to analyze the metagenomic reads: (i) a “Single assemblies” strategy, where assembly and binning was performed for each sample individually. This strategy is known to produce less fragmented assemblies with a limitation of chimeric contigs formation [73]. (ii) a co-assembly strategy was also performed to complete the results with

additional likely lower abundant MAGs. The idea is to pool all the available samples reads and build a unique and common assembly for all samples. Six samples from 2 experiments were used: one with sequences obtained at 2g/L salinity (in +N and -N conditions, no replicate) and the other one at 20 g/L salinity with duplicates for each of the two conditions. Both datasets are similar.

Single assembly strategy

DNA raw reads were analyzed using a dedicated metagenomic pipeline ATLAS v2.7[73]. This tool includes four major steps of shotgun analysis: quality control of the raw reads, assembly, binning, taxonomic and functional annotations. Briefly, quality control of raw sequences is performed using utilities in the BBTools suite (https://sourceforge.net/projects/bbmap/): BBDuk for trimming and removing adapters, BBSplit for decontamination. In our case *Phaeodactylum tricornutum* reference genome (accession GCA_000150955.2), including mitochondria and chloroplast sequences, was used for this specific step. Quality-control (QC) reads assemblies were performed using metaSPADES[74] with ATLAS default parameters. The assembled contigs shorter than 500 bases length and without mapped reads were removed to keep high-quality contigs.

Metagenome-assembled genomes (MAGs) were obtained using two distinct binners : maxbin2[75] and metabat2[76]. The bins obtained by the different binning tools were combined using DASTool[77] and dereplicated with dRep[78] using default parameters. Completeness and contamination were computed using CheckM[79]. Only bins with a completeness above 50 % and a contamination rate under 10 % were kept. Prediction of open reading frames (ORFs) was performed, at the assembly level (not only at the MAGs level) using Prodigal[80]. Linclust[81] was used to cluster the translated gene product obtained to generate gene and protein catalogs common to all samples.

Co-assembly strategy

QC reads and co-assembly were analyzed using a shotgun dedicated sequential pipeline MetaWRAP v1.3.2[77]. Briefly, QC reads are pulled together and addressed to the chosen assembler metaSPAdes[74] using MetaWRAP default parameters. Metagenome-assembled genomes (MAGs) were obtained using two distinct binners: maxbin2 and metabat2 and the bins obtained were combined using an internal MetaWRAP dedicated tool. Completeness and contamination were computed using CheckM[79]. Only bins with a completeness above 50 % and a contamination rate under 10 % were kept. MetaWRAP also includes a re-assemble bins

module that collect reads belonging to each bin, and then reassemble them independently with a "permissive" and a "strict" algorithm. Only improved bins are kept in the final set. Using this strategy, we were able to add an additional MAG.

MAGs relative abundances

The QC reads were mapped back to the contigs, and bam files were generated to organize downstream analysis. Median coverage of the genomes was computed to evaluate MAGs relative abundance estimations.

Taxonomic assignation of metagenomic data

We utilized anvio version 7.2[29] for taxonomic profiling of the *P. tricornutum* associated metagenomes in nitrate deplete and replete condition. The workflow uses The Genome Taxonomy Database (GTDB)[23] to determine the taxanomy based on 22 single copy core genes (scgs, anvio/anvio/data/misc/SCG_TAXONOMY). Sequence alignment search was done using DIAMOND [82].

Hybrid assembly of MAGs

Assembly

Metagenomic assembly of Illumina technology reads does not yield complete genomes due to the difficulty of assembling repetitive regions [83]. Whenever Illumina and PacBio reads were available, we used a strategy to improve MAGs assembly by combining both type of reads. Metagenomic assembly of Illumina paired-end and PacBio reads post quality trimming were assembled using metaSPAdes [74] or SPAdes(v3.15.5) with option flag (--meta). To validate the newly assembled genomes, we verified that the long reads covered regions that were not supported by the mapped Illumina sequences only and that we get high quality bins. We obtained more contiguous genomes in which some regions had not been supported by the assembly of Illumina reads only.

Binning

The contigs were grouped and assigned to the individual genome. To do this, we used MaxBin2 and MetaBAT2 which are clustering methods based on compositional features or on alignment (similarity), or both[84].

Refinement

Bins from MaxBin2 and MetaBAT2 were consolidated into one more solid set of bins. To do

this we used Binning_refiner which improves genomic bins by combining different binning programs available at: https://github.com/songweizhi/Binning_refiner [85].

Taxonomic Assignation

GTDB-Tk has already been independently and positively evaluated for the classification of MAGs[86]. After consolidating the bins in the refinement step, we determined the taxonomy of each bin. The gtdbtk classify_wf module was used in this work using a GTDB database https://github.com/ecogenomics/gtdbtk [87].

Gene annotation of metagenomic data and MAGs

Gene annotation of metagenomics data in two conditions was done using anvi'o version 7.2. Three databases were used for a robust gene observations: COG20[88], KEGG[89] and Prokka (https://github.com/tseemann/prokka). DIAMOND was used to search NCBI's Database. In built, anvi'o program annotates a contig database with HMM hits from KOfam, a database of KEGG Orthologs (KOs, https://www.genome.jp/kegg/ko.html). For Prokka, the annotation was done externally and the gene calls were imported to anvi'o platform for the individual metagenome contigs databases.

Phylogenomic analysis of MAGs

The phylogenomic tree was built using anvi'o -7.1 with database of 1888 TARA ocean MAGs (contig-level FASTA files) submitted to Genoscope (https://www.genoscope.cns.fr/tara/). Additional closest terrestrial and marine genomes (Supplementary Table 6) to the individual MAGs were selected using MicroScope database (https://mage.genoscope.cns.fr/microscope/) using genome clustering, utilizing MASH [90] for ANI (Average nucleotide identity) for calculating pairwise genomic distancing, neighbor-joining (https://www.npmjs.com/package/neighbor-joining) for tree-construction and computing the clustering using Louvain Community Detection (https://github.com/taynaud/python-louvain). anvi'o utilizes 'Prodigal'[80] to identify open reading frames for the contig database. The HMM profiling for 71 single core-copy bacterial genes (SCGs) is done using in-built anvi'o database, Bacteria_71 (https://doi.org/10.1093/bioinformatics/btz188) and utilizes MUSCLE[91] for sequence multiple alignment. The bootstrap values are represented from 0 – 1 with replicates of 100.

Plasmid prediction and annotation

Plasmids were predicted from MetaG data using the following plasmid assembly tools: SCAPP[92], metaplasmidSPAdes[93] and PlaScope[94]. Predicted plasmids were annotated using Dfast[95], eggNOG-mapper v2[96] and Prokka 1.14.6[97].

Tara Oceans MAGs biogeography and environmental preferences

Previously reconstructed MAGs from Tara Oceans metagenomes and respective abundance count tables and fasta files were downloaded from open-source released *Tara* Oceans databases at https://www.genoscope.cns.fr/tara/[13, 98]. Data included 2601 MAGs of which 1888 prokaryotes and 713 eukaryotes MAGs in 937 samples at 2 depths (Surface and Deep Chlorophyll Maximum) and 5 size fractions (0.22-3µm, 3-20µm, 0.8-5µm, 20-200µm, 0.8-2000µm, 180-2000µm) [99]. Data included 87 and 38 samples respectively at surface and DCM depths and 6 size fractions (0.22-3µm, 3-20µm, 0.8-5µm, 20-200µm, 180-2000µm).

The biogeographical occurrences of TARA MAGs phylogenetically close to Pt15 were projected onto global maps for both surface and DCM depths, either by grouping the 5 size fractions (Figure 5), or separately by size fraction (fig. S4).

Tara Oceans physico-chemical parameters were downloaded from Pangaea (*38*). MAGs TSS relative abundances were projected and analyzed in relationship with ammonium (µmol/L), chlorophyll A (mg/m3), iron (µmol/L), nitrite (µmol/L), nitrate (µmol/L), phosphate (µmol/L), nitrate/phosphate, oxygen (µmol/kg), salinity (PSS-78), silicate (µmol/L), temperature (°C) and photosynthetically available radiation (mol quanta/m2/day).

Co-occurrence network inference

Co-occurrence network inference was performed using FlashWeave v0.18.0 [100] with Julia v1.5.3, for eukaryotic and prokaryotic Tara MAGs linked to *Pt15* MAGs. To account for the compositional nature of MAGs abundance data, a multiplicative replacement method [101] was applied to replace zeros, and a Centered Log Ratio transformation [102] was applied separately on both prokaryotic and eukaryotic abundance matrices. FlashWeave parameters used were max_k=1, n_obs_min=10, heterogeneous=False and normalize=False.

Availability of data and materials

All data needed to evaluate the conclusions in the paper are present in the paper and/or the Supplementary Materials. All sequencing data and generated assemblies will be available under the BioProject PRJNA923279.

References

1. Moore CM, Mills, M.M., Arrigo, K.R. I. Berman-Frank, L. Bopp, P. W. Boyd, E. D. Galbraith, , R. J. Geider CG, S. L. Jaccard, T. D. Jickells, J. La Roche, T. M. Lenton, N. M. Mahowald, , E. Marañón IM, J. K. Moore, T. Nakatsuka, A. Oschlies, M. A. Saito, T. F. Thingstad, , Ullo ATO: **Processes and patterns of oceanic**

nutrient limitation. *Nature Geoscience* 2013, **6:**701-710.
2. Einsle O, Rees DC: **Structural Enzymology of Nitrogenase Enzymes.** *Chem Rev* 2020, **120:**4969-5004.
3. Kneip C, Lockhart P, Voss C, Maier UG: **Nitrogen fixation in eukaryotes--new models for symbiosis.** *BMC Evol Biol* 2007, **7:**55.
4. Coale TH, Loconte V, Turk-Kubo KA, Vanslembrouck B, Mak WKE, Cheung S, Ekman A, Chen JH, Hagino K, Takano Y, et al: **Nitrogen-fixing organelle in a marine alga.** *Science* 2024, **384:**217-222.
5. Fiore CL, Jarett JK, Olson ND, Lesser MP: **Nitrogen fixation and nitrogen transformations in marine symbioses.** *Trends Microbiol* 2010, **18:**455-463.
6. Cornejo-Castillo FM, Zehr JP: **Hopanoid lipids may facilitate aerobic nitrogen fixation in the ocean.** *Proc Natl Acad Sci U S A* 2019, **116:**18269-18271.
7. Inomura K, Deutsch C, Wilson ST, Masuda T, Lawrenz E, Lenka B, Sobotka R, Gauglitz JM, Saito MA, Prasil O, Follows MJ: **Quantifying Oxygen Management and Temperature and Light Dependencies of Nitrogen Fixation by Crocosphaera watsonii.** *mSphere* 2019, **4**.
8. Inomura K, Wilson ST, Deutsch C: **Mechanistic Model for the Coexistence of Nitrogen Fixation and Photosynthesis in Marine Trichodesmium.** *mSystems* 2019, **4**.
9. Munoz-Marin MDC, Shilova IN, Shi T, Farnelid H, Cabello AM, Zehr JP: **The Transcriptional Cycle Is Suited to Daytime N2 Fixation in the Unicellular Cyanobacterium "Candidatus Atelocyanobacterium thalassa" (UCYN-A).** *mBio* 2019, **10**.
10. Schlesier J, Rohde M, Gerhardt S, Einsle O: **A Conformational Switch Triggers Nitrogenase Protection from Oxygen Damage by Shethna Protein II (FeSII).** *J Am Chem Soc* 2016, **138:**239-247.
11. Bothe H, Tripp HJ, Zehr JP: **Unicellular cyanobacteria with a new mode of life: the lack of photosynthetic oxygen evolution allows nitrogen fixation to proceed.** *Arch Microbiol* 2010, **192:**783-790.
12. Delmont TO, Quince C, Shaiber A, Esen OC, Lee ST, Rappe MS, McLellan SL, Lucker S, Eren AM: **Nitrogen-fixing populations of Planctomycetes and Proteobacteria are abundant in surface ocean metagenomes.** *Nat Microbiol* 2018, **3:**804-813.
13. Delmont TOPK, J.S. Veseli, I., Fuessel, J. Murat Eren, A., Foster, R.A., Bowler, C., Wincker, P., Pelletier, E.: **Heterotrophic bacterial diazotrophs are more abundant than their cyanobacterial counterparts in metagenomes covering most of the sunlit ocean.** *doi: https://doiorg/101101/20210324436778* 2021.
14. Farnelid H, Andersson AF, Bertilsson S, Al-Soud WA, Hansen LH, Sorensen S, Steward GF, Hagstrom A, Riemann L: **Nitrogenase gene amplicons from global marine surface waters are dominated by genes of non-cyanobacteria.** *PLoS One* 2011, **6:**e19223.

15. Moisander PH, Benavides M, Bonnet S, Berman-Frank I, White AE, Riemann L: **Chasing after Non-cyanobacterial Nitrogen Fixation in Marine Pelagic Environments.** *Front Microbiol* 2017, **8:**1736.
16. Harding KJ, Turk-Kubo KA, Mak EWK, Weber PK, Mayali X, Zehr JP: **Cell-specific measurements show nitrogen fixation by particle-attached putative non-cyanobacterial diazotrophs in the North Pacific Subtropical Gyre.** *Nat Commun* 2022, **13:**6979.
17. Geisler E, Bogler A, Rahav E, Bar-Zeev E: **Direct Detection of Heterotrophic Diazotrophs Associated with Planktonic Aggregates.** *Sci Rep* 2019, **9:**9288.
18. Ababou F-E LMF, Cornet-Barthaux V, Taillandier V and Bonnet S: **Composition of the sinking particle flux in a hot spot of dinitrogen fixation revealed through polyacrylamide gel traps.** *Front Mar Sci 10:1290625* 2024.
19. Geisler E, Bogler A, Bar-Zeev E, Rahav E: **Heterotrophic Nitrogen Fixation at the Hyper-Eutrophic Qishon River and Estuary System.** *Front Microbiol* 2020, **11:**1370.
20. Tschitschko B, Esti M, Philippi M, Kidane AT, Littmann S, Kitzinger K, Speth DR, Li S, Kraberg A, Tienken D, et al: **Rhizobia-diatom symbiosis fixes missing nitrogen in the ocean.** *Nature* 2024, **630:**899-904.
21. Sullivan BW, Smith WK, Townsend AR, Nasto MK, Reed SC, Chazdon RL, Cleveland CC: **Spatially robust estimates of biological nitrogen (N) fixation imply substantial human alteration of the tropical N cycle.** *Proc Natl Acad Sci U S A* 2014, **111:**8101-8106.
22. Nagasato C, Terauchi, M., Tanaka, A. and Motomura, T.: **Development and function of plasmodesmata in zygotes of Fucus distichus.** *Botanica Marina* 2015, **58:**229–238.
23. Parks DH, Chuvochina M, Waite DW, Rinke C, Skarshewski A, Chaumeil PA, Hugenholtz P: **A standardized bacterial taxonomy based on genome phylogeny substantially revises the tree of life.** *Nat Biotechnol* 2018, **36:**996-1004.
24. de Lajudie P, Willems A, Nick G, Moreira F, Molouba F, Hoste B, Torck U, Neyra M, Collins MD, Lindstrom K, et al: **Characterization of tropical tree rhizobia and description of Mesorhizobium plurifarium sp. nov.** *Int J Syst Bacteriol* 1998, **48 Pt 2:**369-382.
25. Yang X, Jiang Z, Zhang J, Zhou X, Zhang X, Wang L, Yu T, Wang Z, Bei J, Dong B, et al: **Mesorhizobium alexandrii sp. nov., isolated from phycosphere microbiota of PSTs-producing marine dinoflagellate Alexandrium minutum amtk4.** *Antonie Van Leeuwenhoek* 2020, **113:**907-917.
26. Zhang X, Tong, J., Dong, M., Akhtar, K. and He, B.: **Isolation, identification and characterization of nitrogen fixing endophytic bacteria and their effects on cassava production.** *PeerJ 10: e12677* 2022, **10**.
27. Bostrom KH, Riemann L, Kuhl M, Hagstrom A: **Isolation and gene quantification of heterotrophic N2-fixing bacterioplankton in the Baltic Sea.** *Environ Microbiol* 2007, **9:**152-164.
28. Medigue C, Calteau A, Cruveiller S, Gachet M, Gautreau G, Josso A, Lajus A, Langlois J, Pereira H, Planel R, et al: **MicroScope-an integrated resource for community expertise of gene functions and comparative analysis of microbial genomic and metabolic data.** *Brief Bioinform* 2019, **20:**1071-1084.
29. Eren AM, Kiefl E, Shaiber A, Veseli I, Miller SE, Schechter MS, Fink I, Pan JN, Yousef M, Fogarty EC, et al: **Community-led, integrated, reproducible multi-omics with anvi'o.** *Nat Microbiol* 2021, **6:**3-6.
30. Lesser MP, Morrow KM, Pankey SM, Noonan SHC: **Diazotroph diversity and nitrogen fixation in the coral Stylophora pistillata from the Great Barrier Reef.** *ISME J* 2018, **12:**813-824.
31. Videira SS, de Araujo JL, Rodrigues Lda S, Baldani VL, Baldani JI: **Occurrence and diversity of nitrogen-fixing Sphingomonas bacteria associated with rice plants grown in Brazil.** *FEMS Microbiol Lett* 2009, **293:**11-19.
32. Skorupska A, Janczarek M, Marczak M, Mazur A, Krol J: **Rhizobial exopolysaccharides: genetic control and symbiotic functions.** *Microb Cell Fact* 2006, **5:**7.

955 33. Hernandez JA, Igarashi RY, Soboh B, Curatti L, Dean DR, Ludden PW, Rubio LM: **NifX and**
956 **NifEN exchange NifB cofactor and the VK-cluster, a newly isolated intermediate of the iron-**
957 **molybdenum cofactor biosynthetic pathway.** *Mol Microbiol* 2007, **63:**177-192.
958 34. Jasniewski AJ, Lee CC, Ribbe MW, Hu Y: **Reactivity, Mechanism, and Assembly of the**
959 **Alternative Nitrogenases.** *Chem Rev* 2020, **120:**5107-5157.
960 35. Wang T, Fu G, Pan X, Wu J, Gong X, Wang J, Shi Y: **Structure of a bacterial energy-coupling**
961 **factor transporter.** *Nature* 2013, **497:**272-276.
962 36. Geiger O, Lopez-Lara IM: **Rhizobial acyl carrier proteins and their roles in the formation of**
963 **bacterial cell-surface components that are required for the development of nitrogen-fixing**
964 **root nodules on legume hosts.** *FEMS Microbiol Lett* 2002, **208:**153-162.
965 37. Cook AM, Denger K: **Metabolism of taurine in microorganisms: a primer in molecular**
966 **biodiversity?** *Adv Exp Med Biol* 2006, **583:**3-13.
967 38. Boutte CC, Crosson S: **Bacterial lifestyle shapes stringent response activation.** *Trends*
968 *Microbiol* 2013, **21:**174-180.
969 39. Stuffle EC, Johnson MS, Watts KJ: **PAS domains in bacterial signal transduction.** *Curr Opin*
970 *Microbiol* 2021, **61:**8-15.
971 40. Madigan M, Cox SS, Stegeman RA: **Nitrogen fixation and nitrogenase activities in members**
972 **of the family Rhodospirillaceae.** *J Bacteriol* 1984, **157:**73-78.
973 41. Singh RK, Singh P, Sharma A, Guo D-J, Upadhyay SK, Song Q-Q, Verma KK, Li D-P, Malviya MK,
974 Song X-P, et al: **Unraveling Nitrogen Fixing Potential of Endophytic Diazotrophs of Different**
975 **Saccharum Species for Sustainable Sugarcane Growth.** *International Journal of Molecular*
976 *Sciences* 2022, **23:**6242.
977 42. Sellstedt A, Richau, K.H.: **Aspects of nitrogen-fixing Actinobacteria, in particular free-living**
978 **and symbiotic Frankia.** *FEMS Microbiology Letters* 2013, **342:**179–186.
979 43. Pesant S, Not F, Picheral M, Kandels-Lewis S, Le Bescot N, Gorsky G, Iudicone D, Karsenti E,
980 Speich S, Trouble R, et al: **Open science resources for the discovery and analysis of Tara**
981 **Oceans data.** *Sci Data* 2015, **2:**150023.
982 44. Karsenti E, Acinas SG, Bork P, Bowler C, De Vargas C, Raes J, Sullivan M, Arendt D, Benzoni F,
983 Claverie JM, et al: **A holistic approach to marine eco-systems biology.** *PLoS biology* 2011,
984 **9:**e1001177.
985 45. Menemenlis BD, Campin, J., Heimbach, P., Hill, C., & Lee, T., 31(October), 13–21. : **ECCO2:**
986 **High resolution global ocean and sea ice data synthesis.** *Mercator Ocean Quarterly*
987 *Newsletter* 2008, **31:**13-21.
988 46. Ward BA DS, Moore CM, Follows MJ.: **Iron, phosphorus, and nitrogen supply ratios define**
989 **the biogeography of**

990 **nitrogen fixation. .** *Limnol Oceanogr* 2013, **58:**2059–2075.
991 47. Bombar D, Paerl RW, Riemann L: **Marine Non-Cyanobacterial Diazotrophs: Moving beyond**
992 **Molecular Detection.** *Trends Microbiol* 2016, **24:**916-927.
993 48. Mohr W, Grosskopf T, Wallace DW, LaRoche J: **Methodological underestimation of oceanic**
994 **nitrogen fixation rates.** *PLoS One* 2010, **5:**e12583.
995 49. Hamersley R TK, Leinweber A, Gruber N, Zehr JP et al . : **Nitrogen fixation within the water**
996 **column associated with two hypoxic basins within the Southern California Bight.** *Aquat*
997 *Microb Ecol* 2011, **63:**193–205.
998 50. Farnelid H, Bentzon-Tilia M, Andersson AF, Bertilsson S, Jost G, Labrenz M, Jurgens K,
999 Riemann L: **Active nitrogen-fixing heterotrophic bacteria at and below the chemocline of**
1000 **the central Baltic Sea.** *ISME J* 2013, **7:**1413-1423.
1001 51. Fernandez C, Farias L, Ulloa O: **Nitrogen fixation in denitrified marine waters.** *PLoS One*
1002 2011, **6:**e20539.
1003 52. Pelusi A, Ambrosino L, Miralto M, Chiusano ML, Rogato A, Ferrante MI, Montresor M: **Gene**
1004 **expression during the formation of resting spores induced by nitrogen starvation in the**
1005 **marine diatom Chaetoceros socialis.** *BMC Genomics* 2023, **24:**106.

1006 53. Takeuchi T, Benning C: **Nitrogen-dependent coordination of cell cycle, quiescence and TAG**
1007 **accumulation in Chlamydomonas.** *Biotechnol Biofuels* 2019, **12:**292.
1008 54. Wang G, Huang L, Zhuang S, Han F, Huang Q, Hao M, Lin G, Chen L, Shen B, Li F, et al: **Resting**
1009 **cell formation in the marine diatom Thalassiosira pseudonana.** *New Phytol* 2024, **243:**1347-
1010 1360.
1011 55. Turk-Kubo KA, Mills MM, Arrigo KR, van Dijken G, Henke BA, Stewart B, Wilson ST, Zehr JP:
1012 **UCYN-A/haptophyte symbioses dominate N(2) fixation in the Southern California Current**
1013 **System.** *ISME Commun* 2021, **1:**42.
1014 56. Carpenter EJ, Janson S: **Intracellular Cyanobacterial Symbionts in the Marine Diatom**
1015 **Climacodium Frauenfeldianum (Bacillariophyceae).** *J Phycol* 2000, **36:**540-544.
1016 57. Janson S, Wouters J, Bergman B, Carpenter EJ: **Host specificity in the Richelia-diatom**
1017 **symbiosis revealed by hetR gene sequence analysis.** *Environ Microbiol* 1999, **1:**431-438.
1018 58. Prechtl J, Kneip C, Lockhart P, Wenderoth K, Maier UG: **Intracellular spheroid bodies of**
1019 **Rhopalodia gibba have nitrogen-fixing apparatus of cyanobacterial origin.** *Mol Biol Evol*
1020 2004, **21:**1477-1481.
1021 59. Sabra W, Zeng AP, Lunsdorf H, Deckwer WD: **Effect of oxygen on formation and structure of**
1022 **Azotobacter vinelandii alginate and its role in protecting nitrogenase.** *Appl Environ*
1023 *Microbiol* 2000, **66:**4037-4044.
1024 60. Limoli DH, Jones CJ, Wozniak DJ: **Bacterial Extracellular Polysaccharides in Biofilm**
1025 **Formation and Function.** *Microbiol Spectr* 2015, **3**.
1026 61. Paerl HW, Prufert LE: **Oxygen-poor microzones as potential sites of microbial n(2) fixation in**
1027 **nitrogen-depleted aerobic marine waters.** *Appl Environ Microbiol* 1987, **53:**1078-1087.
1028 62. Riemann L, Rahav E, Passow U, Grossart HP, de Beer D, Klawonn I, Eichner M, Benavides M,
1029 Bar-Zeev E: **Planktonic Aggregates as Hotspots for Heterotrophic Diazotrophy: The Plot**
1030 **Thickens.** *Front Microbiol* 2022, **13:**875050.
1031 63. Wang D, Xu A, Elmerich C, Ma LZ: **Biofilm formation enables free-living nitrogen-fixing**
1032 **rhizobacteria to fix nitrogen under aerobic conditions.** *ISME J* 2017, **11:**1602-1613.
1033 64. Maier RJ, Moshiri F: **Role of the Azotobacter vinelandii nitrogenase-protective shethna**
1034 **protein in preventing oxygen-mediated cell death.** *J Bacteriol* 2000, **182:**3854-3857.
1035 65. Brian ACJ, C. W. : **The respiratory system of Azotobacter vinelandii.** *Eur J Biochem* 1971,
1036 **20:**29–35.
1037 66. Chakraborty S, Andersen KH, Visser AW, Inomura K, Follows MJ, Riemann L: **Quantifying**
1038 **nitrogen fixation by heterotrophic bacteria in sinking marine particles.** *Nat Commun* 2021,
1039 **12:**4085.
1040 67. Jorgensen JH, Pfaller, M.A., Carroll, K.C., Funke, G., Landry, M.L., Richter, S.S and Warnock.,
1041 D.W. : *Manual of Clinical Microbiology.* 11th edn. Washington (DC): ASM Press; 2015.
1042 68. Isenberg HD: *Clinical Microbiology Procedures Handbook.* 2nd Edition edn: Amer Society for
1043 Microbiology; 1992.
1044 69. Paudel D, Liu F, Wang L, Crook M, Maya S, Peng Z, Kelley K, Ane JM, Wang J: **Isolation,**
1045 **Characterization, and Complete Genome Sequence of a Bradyrhizobium Strain Lb8 From**
1046 **Nodules of Peanut Utilizing Crack Entry Infection.** *Front Microbiol* 2020, **11:**93.
1047 70. Seitzinger SP, and Garber, J. H. : **Nitrogen-fixation and N-15(2) calibration**

1048 **of the acetylene-reduction assay in coastal marine-sediments. .** *Mar Ecol Progr Ser* 1987, **65–73:**65–
1049 73.
1050 71. Hardy RWF HR, Jackson EK, Burns RC. : **The**

1051 **Acetylene-Ethylene Assay for N2 fixation: laboratory and**

1052 **field evaluation.** *Plant Phys* 1968, **43:**1185–1207.
1053 72. Tanaka A DMA, Amato A, Montsant A, Mathieu B, Rostaing P, Tirichine L & Bowler C. :
1054 **Ultrastructure and Membrane Traffic During Cell Division in the Marine Pennate Diatom**
1055 **Phaeodactylum tricornutum.** *Protist* 2015, **166:**506-521

1056 73. Kieser S, Brown J, Zdobnov EM, Trajkovski M, McCue LA: **ATLAS: a Snakemake workflow for**
1057 **assembly, annotation, and genomic binning of metagenome sequence data.** *BMC*
1058 *Bioinformatics* 2020, **21:**257.
1059 74. Nurk S, Meleshko D, Korobeynikov A, Pevzner PA: **metaSPAdes: a new versatile**
1060 **metagenomic assembler.** *Genome Res* 2017, **27:**824-834.
1061 75. Wu YW, Simmons BA, Singer SW: **MaxBin 2.0: an automated binning algorithm to recover**
1062 **genomes from multiple metagenomic datasets.** *Bioinformatics* 2016, **32:**605-607.
1063 76. Kang DD, Li F, Kirton E, Thomas A, Egan R, An H, Wang Z: **MetaBAT 2: an adaptive binning**
1064 **algorithm for robust and efficient genome reconstruction from metagenome assemblies.**
1065 *PeerJ* 2019, **7:**e7359.
1066 77. Sieber CMK, Probst AJ, Sharrar A, Thomas BC, Hess M, Tringe SG, Banfield JF: **Recovery of**
1067 **genomes from metagenomes via a dereplication, aggregation and scoring strategy.** *Nat*
1068 *Microbiol* 2018, **3:**836-843.
1069 78. Olm MR, Brown CT, Brooks B, Banfield JF: **dRep: a tool for fast and accurate genomic**
1070 **comparisons that enables improved genome recovery from metagenomes through de-**
1071 **replication.** *ISME J* 2017, **11:**2864-2868.
1072 79. Parks DH, Imelfort M, Skennerton CT, Hugenholtz P, Tyson GW: **CheckM: assessing the**
1073 **quality of microbial genomes recovered from isolates, single cells, and metagenomes.**
1074 *Genome Res* 2015, **25:**1043-1055.
1075 80. Hyatt D, Chen GL, Locascio PF, Land ML, Larimer FW, Hauser LJ: **Prodigal: prokaryotic gene**
1076 **recognition and translation initiation site identification.** *BMC Bioinformatics* 2010, **11:**119.
1077 81. Steinegger M, Soding J: **Clustering huge protein sequence sets in linear time.** *Nat Commun*
1078 2018, **9:**2542.
1079 82. Buchfink B, Xie C, Huson DH: **Fast and sensitive protein alignment using DIAMOND.** *Nat*
1080 *Methods* 2015, **12:**59-60.
1081 83. Giguere DJ, Bahcheli, A.T., Joris, B.R., Paulssen, J.M., Gieg, L.M., Flatley, M.W., Gloor, G.B.:
1082 **Complete and validated genomes from a metagenome.** *doi:*
1083 *https://doiorg/101101/20200408032540* 2020.
1084 84. Meyer F, Lesker TR, Koslicki D, Fritz A, Gurevich A, Darling AE, Sczyrba A, Bremges A,
1085 McHardy AC: **Tutorial: assessing metagenomics software with the CAMI benchmarking**
1086 **toolkit.** *Nat Protoc* 2021, **16:**1785-1801.
1087 85. Song WZ, Thomas T: **Binning_refiner: improving genome bins through the combination of**
1088 **different binning programs.** *Bioinformatics* 2017, **33:**1873-1875.
1089 86. Coil DA, Jospin G, Darling AE, Wallis C, Davis IJ, Harris S, Eisen JA, Holcombe LJ, O'Flynn C:
1090 **Genomes from bacteria associated with the canine oral cavity: A test case for automated**
1091 **genome-based taxonomic assignment.** *PLoS One* 2019, **14:**e0214354.
1092 87. Chaumeil PA, Mussig AJ, Hugenholtz P, Parks DH: **GTDB-Tk: a toolkit to classify genomes**
1093 **with the Genome Taxonomy Database.** *Bioinformatics* 2019.
1094 88. Galperin MY, Makarova KS, Wolf YI, Koonin EV: **Expanded microbial genome coverage and**
1095 **improved protein family annotation in the COG database.** *Nucleic Acids Res* 2015, **43:**D261-
1096 269.
1097 89. Kanehisa M, Goto S: **KEGG: kyoto encyclopedia of genes and genomes.** *Nucleic Acids Res*
1098 2000, **28:**27-30.
1099 90. Ondov BD, Treangen TJ, Melsted P, Mallonee AB, Bergman NH, Koren S, Phillippy AM: **Mash:**
1100 **fast genome and metagenome distance estimation using MinHash.** *Genome Biol* 2016,
1101 **17:**132.
1102 91. Edgar RC: **MUSCLE: multiple sequence alignment with high accuracy and high throughput.**
1103 *Nucleic Acids Res* 2004, **32:**1792-1797.
1104 92. Pellow D, Zorea A, Probst M, Furman O, Segal A, Mizrahi I, Shamir R: **SCAPP: an algorithm for**
1105 **improved plasmid assembly in metagenomes.** *Microbiome* 2021, **9:**144.
1106 93. Antipov D, Raiko M, Lapidus A, Pevzner PA: **Plasmid detection and assembly in genomic and**
1107 **metagenomic data sets.** *Genome Res* 2019, **29:**961-968.

94. Royer G, Decousser JW, Branger C, Dubois M, Medigue C, Denamur E, Vallenet D: **PlaScope: a targeted approach to assess the plasmidome from genome assemblies at the species level.** *Microb Genom* 2018, **4**.
95. Tanizawa Y, Fujisawa T, Kaminuma E, Nakamura Y, Arita M: **DFAST and DAGA: web-based integrated genome annotation tools and resources.** *Biosci Microbiota Food Health* 2016, **35:**173-184.
96. Cantalapiedra CP, Hernandez-Plaza A, Letunic I, Bork P, Huerta-Cepas J: **eggNOG-mapper v2: Functional Annotation, Orthology Assignments, and Domain Prediction at the Metagenomic Scale.** *Mol Biol Evol* 2021.
97. Seemann T: **Prokka: rapid prokaryotic genome annotation.** *Bioinformatics* 2014, **30:**2068-2069.
98. Delmont T, Gaia, M., Hinsinger DD., et. al. : **Functional repertoire convergence of distantly related eukaryotic plankton lineages revealed by genome-resolved metagenomics.** *Cell Genomics* 2022, **2**.
99. Delmont TO, Pierella Karlusich JJ, Veseli I, Fuessel J, Eren AM, Foster RA, Bowler C, Wincker P, Pelletier E: **Heterotrophic bacterial diazotrophs are more abundant than their cyanobacterial counterparts in metagenomes covering most of the sunlit ocean.** *ISME J* 2022, **16:**927-936.
100. Tackmann J, Matias Rodrigues JF, von Mering C: **Rapid Inference of Direct Interactions in Large-Scale Ecological Networks from Heterogeneous Microbial Sequencing Data.** *Cell Syst* 2019, **9:**286-296 e288.
101. Fernández JAM, Vidal, C.B.& Glahn, V.P. : **Dealing with Zeros and Missing Values in Compositional Data Sets Using Nonparametric Imputation.** *Mathematical Geology* 2003, **35:** pages253–278.
102. Quinn TP, Erb I, Gloor G, Notredame C, Richardson MF, Crowley TM: **A field guide for the compositional analysis of any-omics data.** *Gigascience* 2019, **8**.

Acknowledgements

We acknowledge Clara Guillouche and Irene Romero Rodriguez for their technical assistance with PCR screening and Romain le Balch for his help with GC runs. LT acknowledges support from the region of Pays de la Loire (ConnecTalent EPIALG project), Epicycle ANR project (ANR-19-CE20- 0028-02) and µAlgaNIF France-Japan International Research Project. UC was supported by grant 998UMR6286 Connect Talent EpiAlg from Région Pays de la Loire to LT. SC acknowledges support from the CNRS MITI through the interdisciplinary program *Modélisation du Vivant* (GOBITMAP grant), and the H2020 European Commission project AtlantECO (award number 862923). We are grateful to the bioinformatics core facility of Nantes University (BiRD Biogenouest) for its technical support. The LABGeM (CEA/Genoscope &CNRS UMR8030), the France Génomique and French Bioinformatics Institute national infrastructures (funded as part of Investissement d'Avenir program managed by Agence Nationale pour la recherche, contrats ANR-10-INBS-09 and ANR-11-INBS-0013) are acknowledged for support within the Microscope annotation platform.

Contributions

LT conceived and designed the study. UC performed most of the experiments. SM contributed to the ARA assay and the screening. LJLA assisted with the screening and performed bacterial isolation. TC, CT, EM, UC performed bioinformatics analysis. MG performed bioinformatics analysis and generated figure 5. TL conducted the PON assay. AT performed the EM study. IL assisted with the ARA assay. EJF performed 15N assay. GP supervised EJF and provided guidance on the 15N assay. SC supervised MG. UC, TC, CT, MG, SC, EJF, GP, AT, TL and LT analysed and interpreted the data. LT wrote the manuscript with methodological input from UC, MG, EF, AT, TL, EM and TC. LT supervised and coordinated the study. All authors read, edited and approved the manuscript.

Competing interests

The author(s) declare no competing interest.

Figures and tables legend

Fig. 1. Macro/microscopic phenotype of *P. tricornutum* cells under nitrate starvation. A, A. An illustration comparing the screening results of two P. tricornutum accessions: xenic Pt4 (left), which thrives in +N but does not survive in -N, and the candidate accession, xenic Pt15 (right), shown in duplicates. B, from right to left: axenic Pt15 not surviving in -N (negative control), xenic Pt15 in -N condition and xenic Pt15 transferred to +N medium after 3 months in -N. C-H, micrographs of P. tricornutum xenic cultures on plates. Cells were grown in -N (E, F, H) or +N culture plates (C, D, G). Living cells were observed by DIC (C-F), and fixed cells by transmission electron microscopy (G, H). D, Diatom cells grown in +N possessed yellow-brown color of photosynthetic pigments. Mainly in aggregated cells of fusiform and oval shapes, some bacteria were observed (arrows). D, Single or multiple whitish droplets, oil bodies, were developed next to chloroplasts (arrowheads). E, F, Diatom cells formed aggregates with a significant number of surrounding bacteria (arrows) in the -N culture, compared to the +N condition. F, Diatom cells grown without nitrate also developed oil bodies in the oval cells. G, H, Electron micrographs indicate cross-sectioned cells with or without nitrate. Organelles with high electron density are chloroplast, and major spaces were occupied by oil bodies or vacuoles, which showed low electron densities. Number of bacteria cells (arrows) were obviously larger in -N (H) compared to +N culture (G). H, Interestingly, both Pt cells and some bacteria are encased in sacs surrounded with a likely EPS made membrane (white arrows) which showed darker electron density around diatom cells compared to bacteria. Cells in 1G and 1H were stained with TI blue stain, which binds to negatively charged components such as anionic polysaccharides increasing electron density. A low electron density space (stars) separates Pt cells and bacteria from the membrane. c, chloroplast, v, vacuole, n, nucleus. Scale bars, 10 μm (C-F) and 2 μm (G, H).

Fig. 2. Comparative relative abundance estimation of *Pt15* associated bacteria.

Relative abundance of bacterial community is shown as A, class, B, order, C; family and D, genus (7 most abundant) levels between -N and +N conditions. Taxonomic assignation of metagenomic community associated to *P. tricornutum* in nitrate-deplete and nitrate-replete conditions was done using Anvio version 7.2 standard recommended pipeline using GTDB (The Genome Taxonomy Database) for assigning taxa with the in-built HMM of 22 single copy core genes [23].

Fig. 3. Phylogenetic tree of *Pt15* assembled bacterial genomes amongst 1888 TARA bacterial MAGs and MAGs from MicroScope.

The phylogeny of 71 single copy core genes was built using Anvio platform. The upper circle represents a global view of the phylogeny built using a total of 1927 MAGs and genomes (1888 TARA MAGs, 30 terrestrial MAGs and 9 Pt15 MAGs). The bootstrap values represented from 0 – 1 with replicates of 100 and complete phylogeny can be accessed as an interactive at: https://ncdstree.univ-nantes.fr. The lower part of the figure represents a partial zoom-in on the two clusters where the Pt15 MAGs form groups in the tree with respect to other MAGs and genomes. Cluster A, left (blue highlighted text on the tree) consists of Pt15 associated MAGs: MAG9, MAG4, MAG3, MAG2, MAG8 and MAG21. Cluster B, right (red highlighted text on the tree) consists of Pt15 associated MAGs: MAG7, MAG5 and MAG6. Green highlighted text represents terrestrial bacteria, purple highlighted text represents diazotroph TARA MAGs (reported nifH gene in silico) and non-highlighted text/white background represents non-diazotroph TARA MAGs. Symbol legends, right lower-end denote information with bacterial genomes/MAGs on the tree. (Orange, oval): Pt15 MAGs, (purple, oval): TARA diazotrophic genomes (green oval): MicroScope genomes, (brown, circle): terrestrial bacteria, (blue, circle): marine bacteria, (triangle): symbiotic, (box): free-living, (star): symbiotic and free-living, (inverted triangle): symbiotic and poor- or non-fixer and (circle): no diazotrophic information available. The numbers indicated on the oval symbols correspond to genome information in Table S6.

Fig. 4. Functional gene annotation of *Pt15* associated NCDs in nitrate deplete versus replete conditions. A, Relative abundance of selected genes involved in nitrogen fixation and assimilation in nitrate deplete and nitrate replete conditions. B**,** illustration representing a combined view of 50 top abundant gene in nitrate deplete and replete condition with ordering representing top relatively abundant genes in nitrate deplete conditions. Dashed line indicates the relative percentage at 50%.

Fig. 5. Geographical distribution and ecological relevance of isolated and assembled bacterial diazotrophs genomes correlating to TARA data. Geographical distribution of phylogenetically closest *Pt15* associated TARA Ocean MAGs in A, surface and B, DCM samples. C, D, relative abundance of the top 2 most occurring MAGs of *Pt15* bacterial

community (C, D, *Mesorhizobium* MAG3, E, F *Bradyrhizobium* MAG8 respectively) in the environment in respect to nitrate, oxygen and iron concentrations. F, Co-occurrence of *Pt15* MAGs in the environment with different species of micro-eukaryotes inferred through FlashWeave, FDR <0.01)[100].

Table 1. List of isolated bacteria from xenic *Pt15* in -N condition.

NCDs are indicated in bold. NA, not assembled, ND, not determined.

Supplementary figures and tables legend

Figure S1. Particulate Organic Nitrogen (PON) measurements. a, PON kinetic and b, corresponding xenic *Pt15* biomass for 6 time points over a period of 80 days in nitrate deplete and replete conditions.

Figure S2. Agarose gel pictures of PCR amplified products. A, amplification of *nifH* gene in isolated bacteria using degenerate primers. 1, *Stenotrophomonas maltophilia* MAG20, 2, *Bradyrhizobium* sp. (MAG 21), 3, Positive control (PC) *Azotobacter vinelandii*, Negative control (NC). B, 1, *Paracoccus sp*., 2, *Bradyrhizobium sp.*, (MAG 21), *Azotobacter vinelandii* (PC), Negatice control (NC). A black arrow indicates the *nifH* PCR band.

Figure S3. Phylogenomic tree representing clusters C, D and E MAGs from *Pt15* and other microalgae with 1888 TARA ocean bacterial MAGs.

Figure S4. Geographical distribution of phylogenetically closest *Pt15* associated TARA oceans MAGs in different size fractions from surface and DCM samples.

Figure S5. Relative abundance of the top 2 most occurring MAGs of *Pt15* bacterial community (this study diazo, *Mesorhizobium* MAG3 and *Bradyrhizobium* MAG8) compared to TARA diazotrophic MAGs and non-diazotrophic MAGs in the environment in respect to oxygen in 0.22-1.6/3 µm (A) and 0.8-5 µm (B) size fractions.

Additional File 1. Media recipes used for isolation of bacteria from *Phaeodactylum tricornutum* and other microalgae.

Table S1. Combined table representing amount of ethylene (Acetylene reduction assay), N15 incorporation assay and PON detection in xenic *Pt15* in nitrate deplete condition.

Table S2. Details of taxonomy for bacterial metagenomics data in nitrate deplete and nitrate replete conditions (replicates).

Table S3. MAG features, species-specific plasmid detection from *Pt15* meta-genomic data and TARA MAGs corresponding to Pt15 MAGs.

Table S4. Gene annotation using anvio_COG20, anvio_KEGG and anvio_Prokka of the metagenomics data in nitrate deplete and replete conditions (replicates).

Table S5. Details of Microalgae collection screened in nitrate deplete condition and bacteria isolated from specific microalgae.

Table S6. Features of the genomes selected from Mircoscope for phylogenetic studies.

Table S7. List of primers used in the study.

a

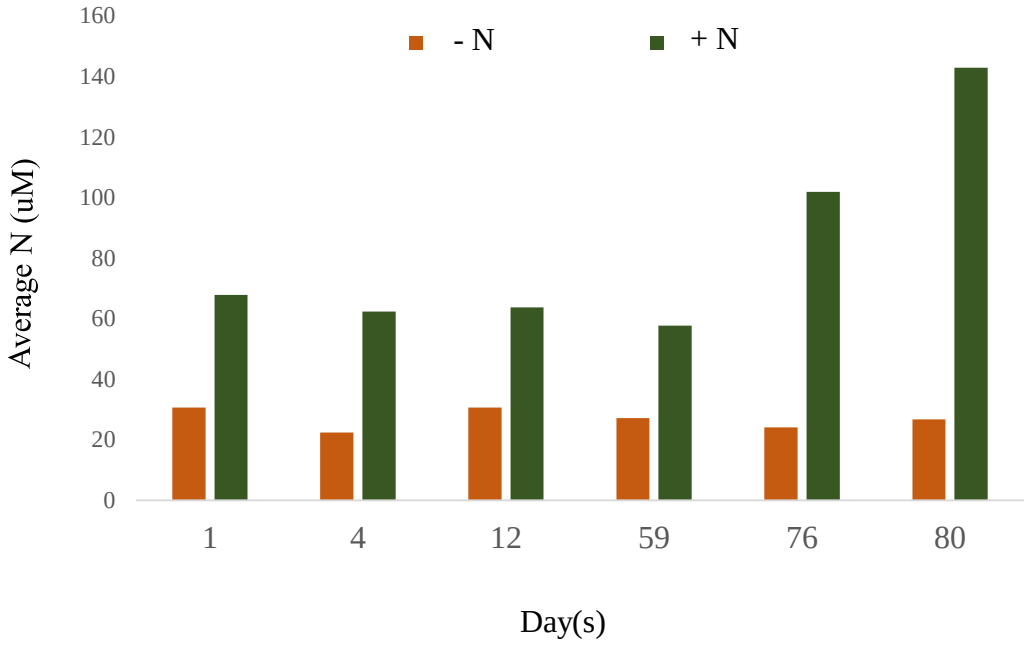
160
140
120
100
80
60
40
20
0
- N
+ N
Average N (uM)
1
4
12
59
76
80
Day(s)

b

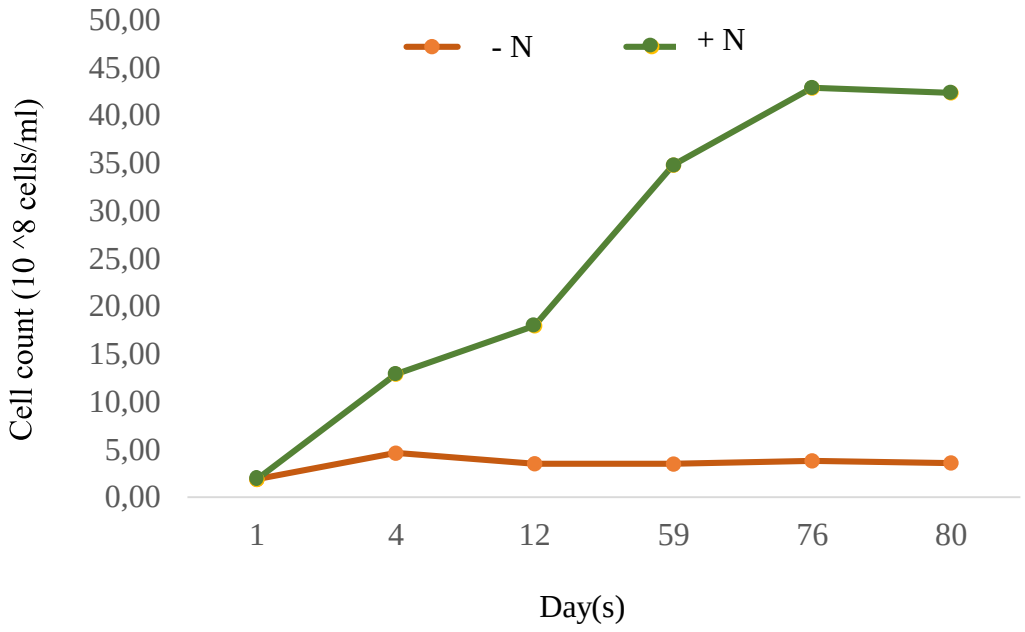
50,00
45,00
40,00
35,00
30,00
25,00
20,00
15,00
10,00
5,00
0,00
- N
+ N
Cell count (10 ^8 cells/ml)
1
4
12
59
76
80
Day(s)

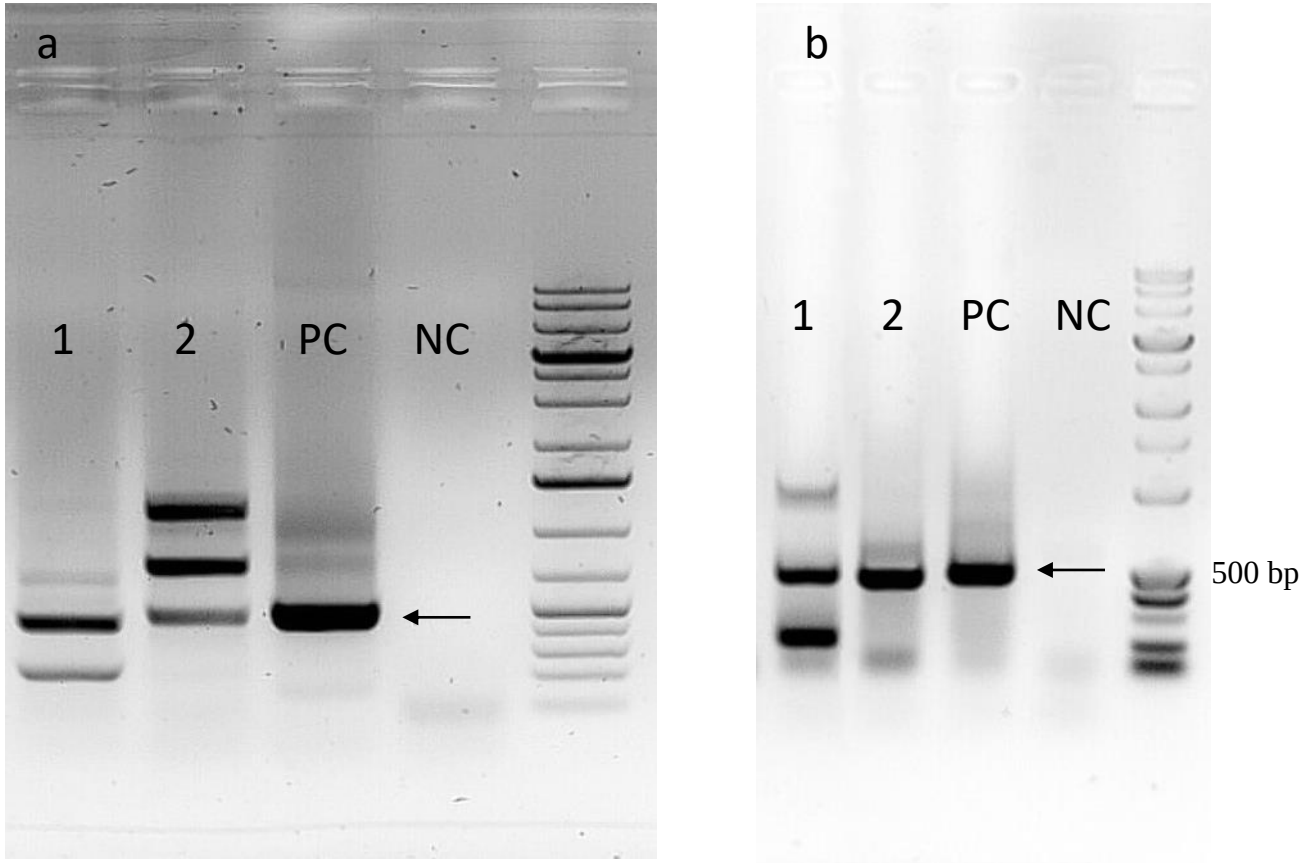
a
1
2
PC
NC
b
1
2
PC
NC
500 bp

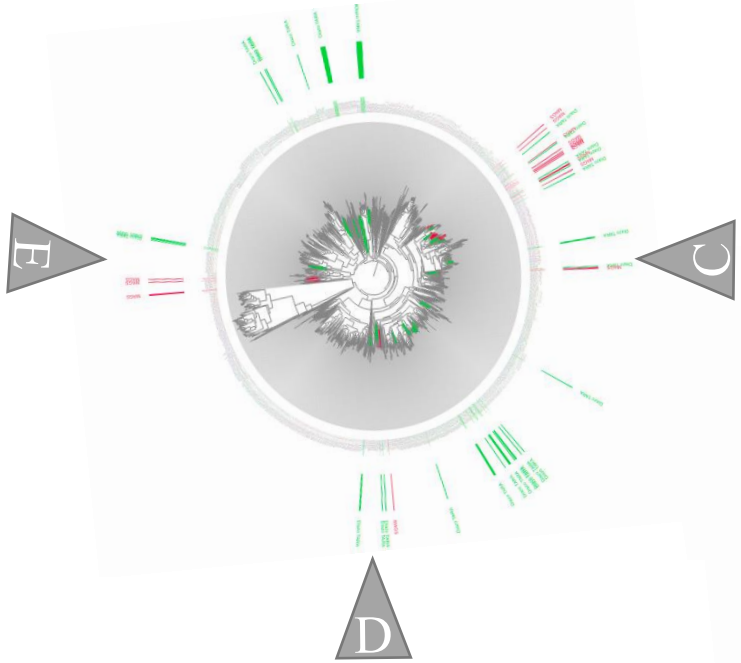

Legend

- Assembled MAGs
- Non-diazotrophic TARA genomes
- Diazotrophic TARA genomes

Cluster C

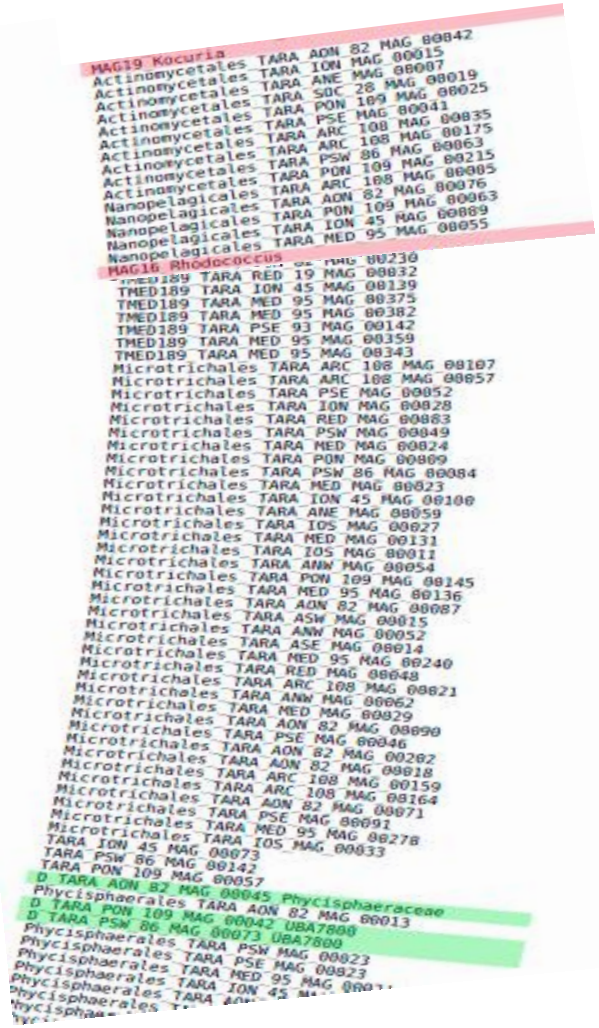

Cluster D

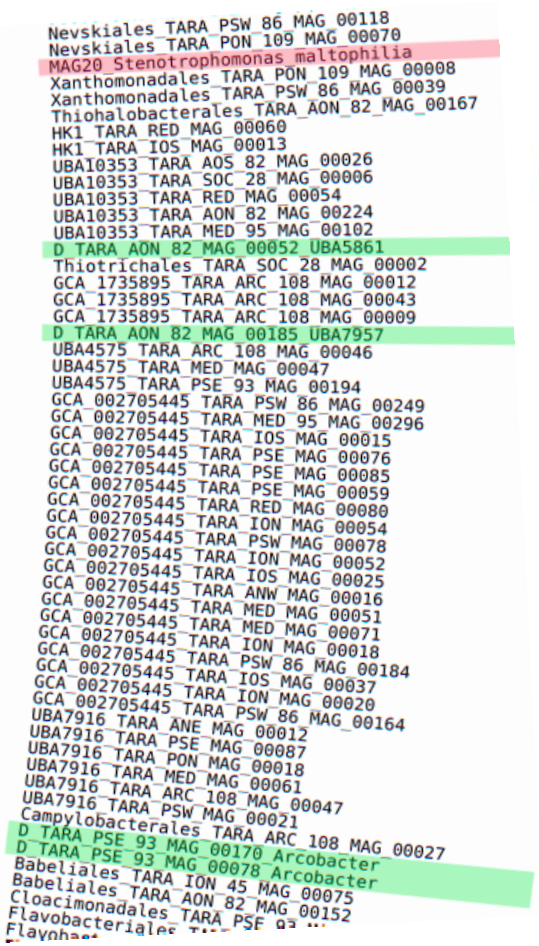

Cluster E

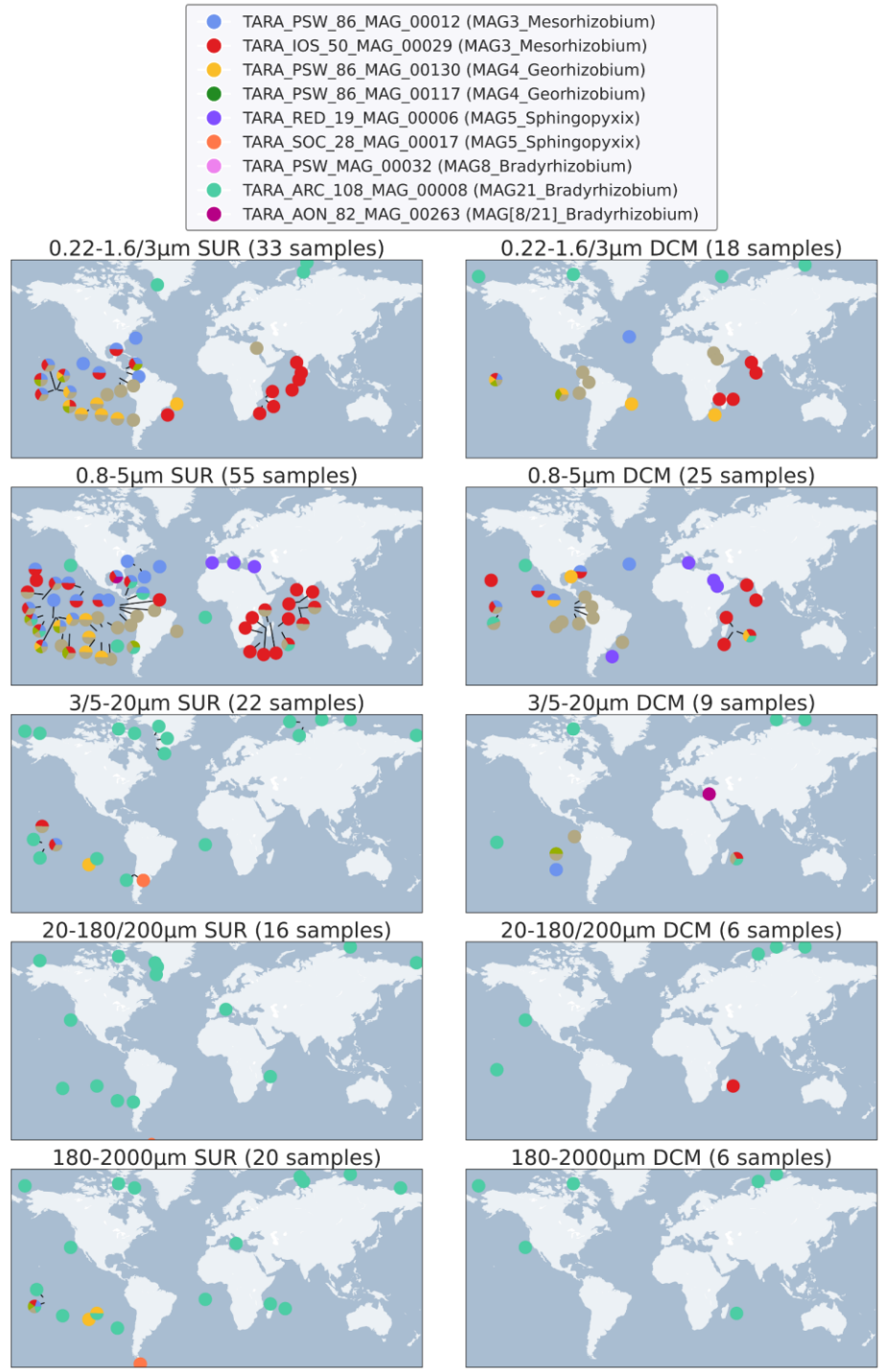
TARA_PSW_86_MAG_00012 (MAG3_Mesorhizobium)
TARA_IOS_50_MAG_00029 (MAG3_Mesorhizobium)
TARA_PSW_86_MAG_00130 (MAG4_Georhizobium)
TARA_PSW_86_MAG_00117 (MAG4_Georhizobium)
TARA_RED_19_MAG_00006 (MAG5_Sphingopyxix)
TARA_SOC_28_MAG_00017 (MAG5_Sphingopyxix)
TARA_PSW_MAG_00032 (MAG8_Bradyrhizobium)
TARA_ARC_108_MAG_00008 (MAG21_Bradyrhizobium)
TARA_AON_82_MAG_00263 (MAG[8/21]_Bradyrhizobium)
0.22-1.6/3µm SUR (33 samples)
0.22-1.6/3µm DCM (18 samples)
0.8-5µm SUR (55 samples)
0.8-5µm DCM (25 samples)
3/5-20µm SUR (22 samples)
3/5-20µm DCM (9 samples)
20-180/200µm SUR (16 samples)
20-180/200µm DCM (6 samples)
180-2000µm SUR (20 samples)
180-2000µm DCM (6 samples)

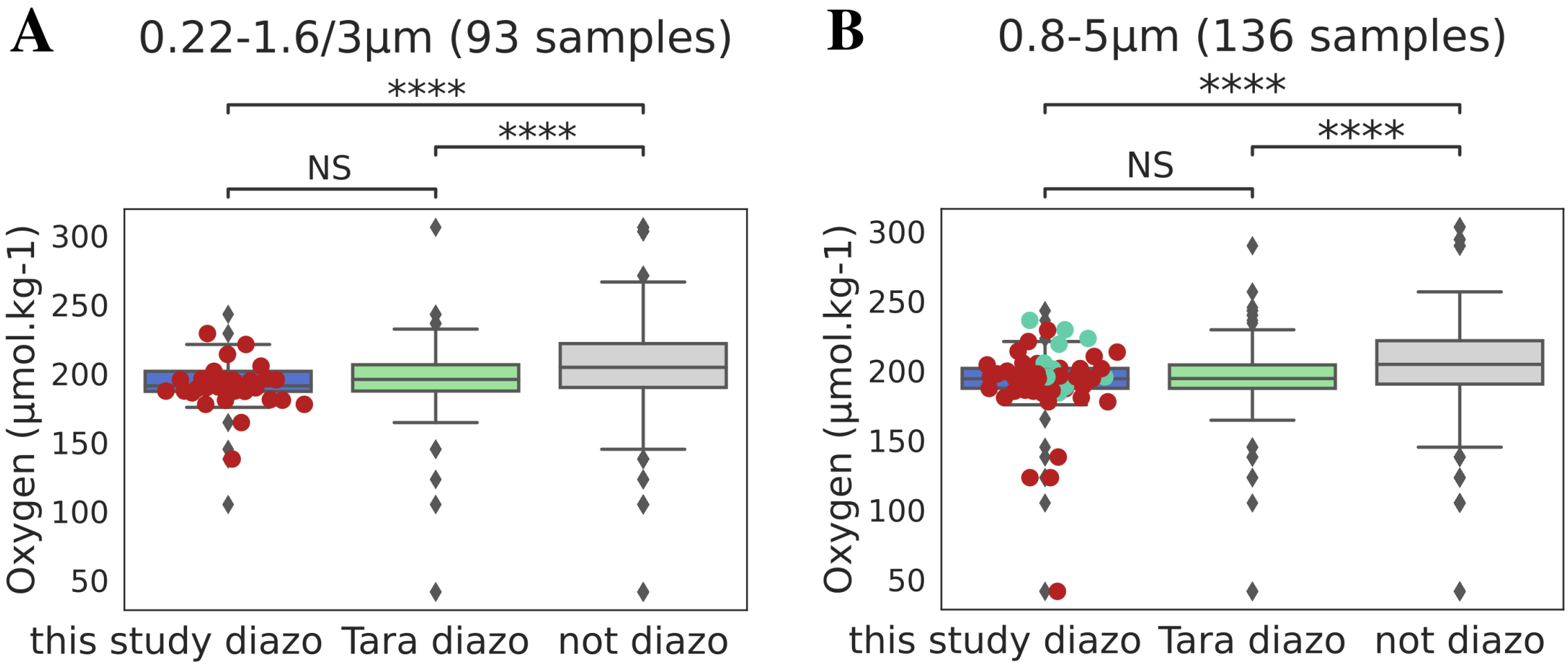
A
0.22-1.6/3µm (93 samples)
****
****
NS
Oxygen (µmol.kg-1)
300
250
200
150
100
50
this study diazo
Tara diazo
not diazo
B
0.8-5µm (136 samples)
****
****
NS
Oxygen (µmol.kg-1)
300
250
200
150
100
50
this study diazo
Tara diazo
not diazo